Master of Science Thesis in Electrical Engineering
Department of Electrical Engineering, Linköping University, 2018

Impact of Engine Dynamics on Optimal Energy Management Strategies for Hybrid Electric Vehicles

Andreas Hägglund and Moa Källgren

LINKÖPING UNIVERSITY

Master of Science Thesis in Electrical Engineering

Impact of Engine Dynamics on Optimal Energy Management Strategies for Hybrid Electric Vehicles

Andreas Hägglund and Moa Källgren

LiTH-ISY-EX--18/5163--SE

Supervisor: **Fatemeh Mohseni**
ISY, Linköpings universitet
Martin Sivertsson
Volvo Car Corporation
Markus Grahn
Volvo Car Corporation
Dhinesh Velmurugan
Volvo Car Corporation

Examiner: **Lars Eriksson**
ISY, Linköpings universitet

Division of Automatic Control
Department of Electrical Engineering
Linköping University
SE-581 83 Linköping, Sweden

Abstract

In recent years, rules and regulations regarding fuel consumption of vehicles and the amount of emissions produced by them are becoming stricter. This has led the automotive industry to develop more advanced solutions to propel vehicles to meet the legal requirements. The Hybrid Electric Vehicle is one of the solutions that is becoming more popular in the automotive industry. It consists of an electrical driveline combined with a conventional powertrain, propelled by either a diesel or petrol engine. Two power sources create the possibility to choose when and how to use the power sources to propel the vehicle. The strategy that decides how this is done is referred to as an energy management strategy. Today most energy management strategies only try to reduce fuel consumption using models that describe the steady state behaviour of the engine. In other words, no reduction of emissions is achieved and all transient behaviour is considered negligible.

In this thesis, an energy management strategy incorporating engine dynamics to reduce fuel consumption and nitrogen oxide emissions have been designed. First, the models that describe how fuel consumption and nitrogen oxide emissions behave during transient engine operation are developed. Then, an energy management strategy is developed consisting of a model predictive controller that combines the equivalent consumption minimization strategy and convex optimization. Results indicate that by considering engine dynamics in the energy management strategy, both fuel consumption and nitrogen oxide emissions can be reduced. Furthermore, it is also shown that the major reduction in fuel consumption and nitrogen oxide emissions is achieved for short prediction horizons.

Acknowledgments

We would first like to thank our thesis advisor Fatemeh Mohseni from the department of electrical engineering at Linköping University for all the valuable inputs on the thesis.

We would also like to thank our supervisors; Martin Sivertsson, Markus Grahn, and Dhinesh Velmurugan at Volvo Cars Corporation for your commitment of being our supervisors. We are grateful for your engagement in the project and for all valuable input you have provided as well as all the interesting discussions. A thank you should also be dedicated to Christoffer Strömberg at Volvo Cars Corporation, thank you for your valuable input about optimization.

We would also like to thank our opponents, Simon Berntsson and Mattias Andreasson, who has given their advice about optimization along the project.

Finally we would like to thank our examiner Lars Eriksson for his expertise and enthusiasm in the subject that have had a considerable positive impact on our studies.

Linköping, June 2018
Andreas Hägglund and Moa Källgren

Contents

Notation

General notations

Variable	Representing
P	Power
T	Torque
F	Force
v	Velocity
ω	Rotational Speed
a	Acceleration
θ	Angle
t	Time

Index notations

Index	Representing
f	Fuel
NOx	Nitrogen oxides
$meas$	Measured values
$stat$	Values from quasi static measurements
act	Actual value at current time step
req	Requested value at current time step
$trans, start$	Start of transient
$trans, end$	End of transient
whl	Wheel
ech	Electrochemical
pt	Power Train
$quad$	Quadratic

Battery notations

Variable	Representing
ξ	State of charge
U_{oc}	Open-circuit voltage
I	Current
R_i	Battery internal resistance
Q	Battery capacity
Q_0	Battery nominal capacity

Optimization notations

Variable	Representing
J	Cost function
λ_{NOx}	Equivalence factor for NOx
λ_{ech}	Equivalence factor for SoC
dt	Sample Time

Constants

Notation	Representing
A_{NOx}	Inclination of the dynamic NOx model
Q_{LHV}	Lower heating value of combustion
a_{SoC}	The inclination for SoC relationship
b_{SoC}	The offset for SoC relationship
α	Scaling factor for variables
β	Scaling factor for equations
γ	Speed ratio between ICE and ISG
$a_{1...n}$	The inclination of the piece-wise linearized models
$b_{1...n}$	The offset of the piece-wise linearized models
a_k	Inclination of dynamic fuel model
$A_{quad,NOx}$	First term of quadratic dynamic NOx model
$B_{quad,NOx}$	Second term of quadratic dynamic NOx model

Abbreviations

Abbreviation	Complete form
HEV	Hybrid Electric Vehicle
ICE	Internal Combustion Engine
EMS	Energy Management Strategy
EM	Electric Machine
ECMS	Equivalent Consumption Minimization Strategy
FTP75	EPA Federal Test Procedure
SoC	State of Charge
DDP	Deterministic Dynamic Programming
PMP	Pontryagin´s Minimum Principle
SDP	Stochastic Dynamic Programming
MPC	Model Predictive Control
EGR	Exhaust Gas Recirculation
VGT	Variable-Geometry Turbocharger
WLTC	Worldwide Harmonized Light vehicles Test Cycles
ISG	Integrated Starter Generator
RMSE	Root Mean Square Error
QCML	Quadratic Cone Modeling Toolbox
ECU	Electronic Control Unit

1 Introduction

1.1 Background

In the last decade, human actions have led to dramatic environmental changes that have devastating consequences on the environment. A rapid increase of green house gases have caused higher temperatures, more extreme weather conditions, rising ocean levels and an increase in air pollution and will continue to do so if no arrangements are made to prevent this. The global population have become more aware of this issue and in response to this awareness, legislation is being passed across the world to ensure these consequences are not irreversible. A major part of this legislation has affected the automotive industry and forced it to adapt and to primarily reduce vehicle emissions and fuel consumption. Recently it has also become clear that the drive cycles used for certifying this legislation does not capture real driving conditions. This has enabled the car industry to optimize their vehicles to pass these simplified drive cycles while not performing as well during real driving conditions. Therefore, tougher driving cycles that capture real driving conditions, both steady-state and transient driving behaviour, are being designed and implemented.

1.2 Problem Description

A popular solution to meet the legislation passed is the Hybrid Electric Vehicle (HEV). One kind of HEV is a car that has an Internal Combustion Engine (ICE) and an Electric Machine (EM). Since the power can be provided from two different actuators it creates the possibility to optimize how and when to engage them, often to ensure low fuel consumption as well as low emissions. To pass the new tests, more complex aftertreatment systems are being designed to ver-

ify legislation concerning emissions. On the other hand, hybridization enables minimization of both emissions and fuel consumption at the same time if good control systems are available. Recent studies, see [1–3], has also shown that encapsulating the dominating dynamics of the powertrain in the powertrain model could result in even lower fuel consumption and emissions. The HEV is increasingly becoming popular because it does not only pass the tougher driving cycles, it also performs better in real life.

To be able to utilize the full potential of HEVs, it is necessary to look at the Energy Management Strategy (EMS). The EMS developed in this thesis determines how the torque required by the driver should be split between the two energy sources in order to ensure low fuel consumption and low emissions while maximizing power utilization. The EMS can be formulated in very different ways depending on the requirements of a specific application [4].

In this master thesis, an optimal energy management strategy will be constructed for a mild parallel HEV that is charge sustaining. Charge sustaining means that the battery level should be the same at the end of the drive cycle as it was at the beginning. The long term goal of the method developed in this thesis is to be implemented as a real time optimal controller. A real time optimization method optimizes the given problem in real time which therefore, puts constraints on the complexity of the problem as well as the computational time of the optimization technique. A common strategy to meet these requirements is to view the problem as a series of stationary operating points. However, this does neglect the transition cost from one operating point to another. Therefore, models accounting for actuator dynamics will be designed and implemented. Then, an optimization strategy with low computational complexity and short term prediction horizon will be designed to minimize the fuel consumption as well as the amount of nitrogen oxides, NOx, emissions before the after treatment system. The final EMS will be implemented and compared to optimization strategies using only static models. The length of the prediction horizon will be analyzed to see how it affects the results.

The studied vehicle is a mild parallel hybrid which is based on an ICE that runs on diesel with an additional electric path. In parallel hybrids, both the combustion engine and the electric machine can supply the desired power, alone or in combination, which makes it possible to optimize the EMS between the two parallel paths [5]. Figure 1.1 illustrates the studied parallel HEV powertrain configuration. The Integrated Starter Generator (ISG) acts as an electric machine.

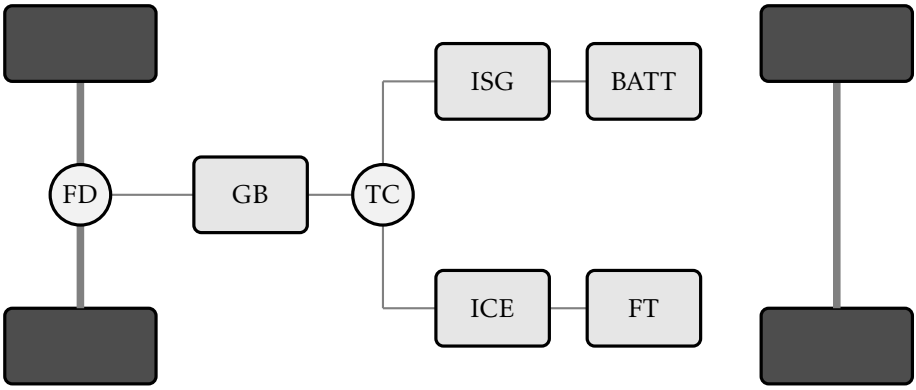

Figure 1.1: *An illustration of a parallel HEV which contains the components final drive (FD), a gearbox (GB), a torque coupler (TC), an internal combustion engine (ICE), a fuel tank (FT), an integrated starter generator (ISG), and a battery (BATT). The darker rectangles represents the wheels of the vehicle.*

1.3 Literature Review

This section presents a short review of recent research studies on the topic of this thesis.

1.3.1 Optimization strategies

There are several different optimization-based EMS and a common goal for all of them is to minimize some predefined state variables and the most common one is fuel consumption. This is done by minimizing an objective function that depend on these variables. The main control optimization based strategies are represented in Figure 1.2. Rule-based control strategies are used for controlling fundamental control schemes, and optimization-based control strategies minimize an objective function [4]. The optimization-based control techniques can be further divided in to real-time and global optimization methods.

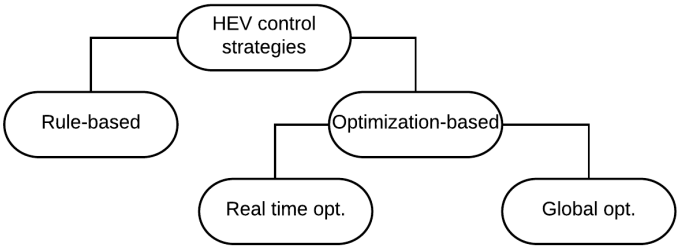

Figure 1.2: *Overview of HEV control strategies.*

The global optimization strategies have the advantage of finding the global optimum by optimizing the complete powertrain system, given complete knowledge of a drive cycle. Two common techniques that are used for this purpose are linear programming and dynamic programming. The reader is referred to [4] for more details about these two techniques. The downside with these techniques are that they are computationally heavy and are not suitable for real-time applications. However, they are useful for validating real-time optimization strategies.

Real-time optimization methods reduce the size of the optimization problem by introducing an instantaneous objective function that depend only on the present state variables. Then, a local optimum is calculated instantaneously at each time step during a driving mission. Most of the real-time optimization strategies and the local optimum calculations do not necessarily give a global optimum but they often give a solution close to the global optimum. Some of the common techniques that have been used in literature are Pontryagin's Minimum Principle (PMP) [6, 7], Equivalent Consumption Minimization Strategy (ECMS) [8, 9], and Model Predictive Control (MPC) [3]. In both [8, 9], an ECMS has been applied

on a parallel hybrid and the results show that both fuel and NOx emissions are reduced compared to other strategies. The results in [6, 7] show that PMP is a good candidate for solving a real-time optimization problem.

MPC is a suitable method for controlling dynamic models. By taking future time into account, MPC optimizes the current timeslot [4]. In [3] an MPC that considers the effects of the diesel-engine transient characteristics is evaluated. These characteristics become more obvious in HEV applications as there are frequent transient operations. Since MPC takes future driving characteristics into account, it could potentially decrease fuel consumption and emissions by incorporating this when calculating the optimal control signals. Therefore, an MPC could have a greater impact when it is applied on a drive cycle with more transient driving behaviour such as rapid accelerations, etc.

Another strategy that has become increasingly popular for optimization of powertrains in HEVs is convex optimization. This is due to its computational efficiency as well as the guarantee of finding a global optimum for a given problem. But, the optimization problem sometimes has discrete decision variables which cannot be optimized by convex optimization. Therefore, a good approach is to use Deterministic Dynamic Programming (DDP) for the discrete variables (engine on/off and gearshifts) and convex optimization to determine the optimal power split. By adding costs for switching the engine off/on and for gearshifts, it prevents the engine from doing unacceptably frequent starts and gear shifts [10]. When this method was compared to a basic DP algorithm, the method resulted in a reduction of evaluation time and a higher precision because the convex optimization does not require a discretization of the state variables and the continuous control. Another downside with convex optimization is that it requires convex models which is not always possible.

1.3.2 Modeling

Research presented in [2, 3, 11–13] has shown that the main difference between steady-state engine operation and transient operation, with respect to emissions and fuel consumption is caused by dynamics in the air system. Since most diesel engines are equipped with a turbo system, it is the inertia of the compressor, turbine, and turbine shaft that cause the dynamic behaviour. Therefore, it is important to consider them when implementing an EMS that considers transient behaviour [12]. Results show that the optimal trajectories differ substantially and that neglecting the turbocharger dynamics can underestimate the consumption by over 60 %. Also the required energy needed to go to the optimal operation points differs from the case in which the dynamics are neglected [11].

If Variable-Geometry Turbocharger (VGT) and Exhaust Gas Recirculation (EGR) are parts to be considered, the EMS model will probably be easily modeled in two parts. The first part calculates the injected fuel, setpoints for boost pressure, oxy-

gen fraction in the intake manifold, and injection timing. Then, the second part considers the VGT and EGR. This is an approach that was used before with good results, see [14]. According to [14], by using an offline based transient EMS on a diesel engine, reduction of fuel consumption and the emission peaks compared to steady-state EMS are achieved for the New European Driving Cycle (NEDC).

NOx is strongly correlated to high temperatures in the cylinder which in turn depends on oxygen concentration and combustion duration. A change of load leads to increased fuelling which in turn makes the control system starve the EGR. Consecutively, this leads to increased NOx emissions as the engine is moving toward the desired working point [13].

Static NOx and fuel models can be acquired from static engine measurements where engine speed and torque are changed in a systematic order [13]. NOx emissions are however very correlated to transient effects. This is because they are very dependent on the temperature in the cylinder which in turn depend on oxygen concentration. During a transient operation, either the engine speed or the torque is changed which results in disturbances in the combustion chamber and air entrapment until steady-state is attained. This behaviour should preferably be captured by the transient models and could be well-described by modelling the turbocharger lag which greatly affects the intake manifold pressure. Therefore, a dynamic model of the intake manifold pressure could be enough to encapsulate turbocharger dynamics. A possible transient NOx model is presented in [2] where the transient part of the model is modeled as a step in engine effect multiplied with a correction factor that depend on the relative cumulative emission mass flow errors. Results indicate that significantly lower emissions are achieved when using the model described with Equation 2 in [2].

The fuel flow can be modeled from the wheel speed and is approximated in [5] as a function of engine friction pressure, engine speed, torque, cylinder volume, lower heating value, Willans efficiency, and time.

1.4 Approach

The work consists of three major parts:

1. Modelling
2. Optimization
3. Analysis

In the modelling part, the models that describe the fuel consumption and the amount of NOx emissions are designed. Two sets of models are developed, static and dynamic. The static models capture only steady-state driving behaviour and the dynamic models capture both the behaviour during steady-state and transient driving conditions. The models are designed based on data used in [13].

In the optimization part, one convex optimization tool is chosen. When a convex optimization strategy is used, it requires the models to be convex. If the designed models are not convex they have to be approximated as convex functions. Other possible optimization strategies are for example non-convex optimization methods and linearization around each working point. These methods have not been investigated in this thesis, instead convex optimization is used because of its advantages mentioned in section 1.3. Further explanation about convex optimization is found in chapter 3.

Finally, global optimization based EMS and real-time optimization based EMS are designed based on the models created. The real-time optimization is validated against the global optimization, with and without the dynamic models and the results are analyzed. To be able to compare the results for the different methods on an even scale of performance the energy management strategies developed are charge sustaining.

1.5 Risks and Delimitations

One of the goals for this thesis is to investigate the impact of the length of a short time prediction horizon on the optimal torque split and thus the fuel consumption and the NOx emissions. To do so, a given driving cycle will be used which means that the velocity profile of the car will be known and therefore, no prediction is actually made. But, this is still a fair delimitation since the goal is to investigate if a potential velocity prediction could yield a better optimization. If the optimization is not improved, trying to predict the velocity to use in an MPC is meaningless.

The developed models are based on data from engine test rigs. How this data was produced is crucial since engine tests are done to produce data that fits a certain application. The data that is used in this thesis was developed for another application with a similar goal, though with a different approach, where a transient NOx model was developed, see [13]. The transient behaviour of this model depend on several variables that were adjusted during the tests. However, the model in this thesis does not depend on these variables and therefore, it might be difficult to extract sufficient information from the given data.

1.6 Thesis goals

This thesis aims to evaluate the impact of engine dynamics on the NOx emissions and fuel consumption. Steady-state models as well as dynamics models for these variables of interest will be designed. Then, they will be integrated with an HEV model and a global EMS as well as a real-time EMS will be developed with the goal to minimize fuel consumption and NOx emissions.

The following questions should be answered:

- Is it possible to save fuel and reduce NOx emissions by considering dynamic actuator behaviour when developing an optimal EMS for a charge sustaining HEV?
- By using a prediction horizon, is it possible to save fuel and reduce NOx emissions, and how does the length of the prediction horizon affect the emissions and fuel consumption?

1.7 Outline

The rest of the report is organized in the following chapters.

2. **The Hybrid Electric Vehicle** - Facts about the HEV and its basic theory
3. **Optimization Strategy** - What strategies is used and theories behind them
4. **Method** - How the models, static and dynamic, are developed as well as how the optimization problem is defined
5. **Validation** - Explanation of how the result is developed
6. **Result** - Presentation of the obtained result
7. **Analyses** - Contains analyses of result
8. **Conclusions and Future Work** - Conclusions are given with a discussion and some suggestions about Future Work

2

The Hybrid Electric Vehicle

To improve performance, lower both fuel consumption and emitted emissions, the Hybrid Electric Vehicle (HEV) is a good alternative to the common combustion engine. The advantages of the HEV are the possibility to downsize the engine, recover some energy during deceleration, optimize the power distribution, eliminate the idle fuel consumption by turning off the combustion engine, and eliminate the clutch losses.

HEVs have two or more prime movers and power sources. In general, an HEV includes an combustion engine as a fuel converter or irreversible prime mover.

An HEV can have different architecture designs; series, parallel, or combined hybrid, where the most common one is the parallel hybrid with a gasoline engine. This thesis will consider a parallel hybrid with a diesel engine, where both prime movers operate on the same drive shaft. Thus, they can power the vehicle individually or simultaneously.

2.1 Series Hybrid

The series hybrid can be seen as an electric vehicle with an additional ICE-based energy path since it is the electric machine that is coupled to the drive shaft. The combustion engine output is converted into electricity that can either directly feed the electric machine or charge the battery and the link between the combustion engine path and the battery is electrical. How the power is distributed through the driveline is determined by the power link which is regulated by the power split controller. Figure 2.1 illustrates the design of a series hybrid.

The advantage of a series hybrid is that the ICE is decoupled from the drive shaft and can be operated with optimal efficiency. There is also no need of a complicated multi-speed transmission or clutch because the engine is decoupled and that the EM does not need them. The disadvantage is that it requires three machines which add some weight and cost to the vehicle. The overall efficiency of using a series hybrid will approximately be the same as for vehicles with modern ICEs.[5]

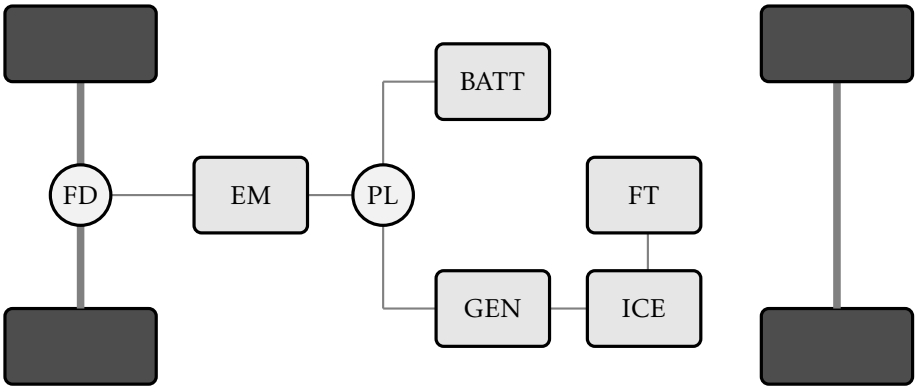

Figure 2.1: *A configuration of a series HEV, which contains the parts final drive (FD), an electric machine (EM), a power link (PL), an internal combustion engine (ICE), a fuel tank (FT), a generator (GEN), and a battery (BATT). The darker rectangles represents the wheels of the vehicle.*

2.2 Parallel hybrid

The parallel hybrid may be considered as a conventional vehicle with an additional electric path. In the parallel hybrid, both prime movers operate on the same drive shaft which make it possible to use the electric and the fuel power individually or simultaneously. This makes it possible to turn the engine on/off and the electric machine can be used to assist during accelerations. The torque coupler distributes the power flow between the actuators and is regulated in an optimal manner by a regulator.

Since only two components are needed, there are weight and cost advantages compared to series hybrids. However there is need for a transmission due to the fact that the ICE is mechanically coupled to the drive shaft, which adds losses to the configuration. Figure 2.2 illustrate the components and schematic picture of the power train of a parallel HEV [5].

There are different ways of positioning the electric machine with respect to the traditional drive train; micro hybrids, pre-transmission parallel hybrid, single-shaft hybrid, post-transmission parallel hybrid, double-shaft parallel hybrid, trough-the-road parallel hybrid, and double-drive parallel hybrid. For more information about these, see [5].

The overall efficiency of a parallel hybrid vehicle will be better than that of a modern ICE based vehicle because of brake energy recuperation and low load electrical operation.

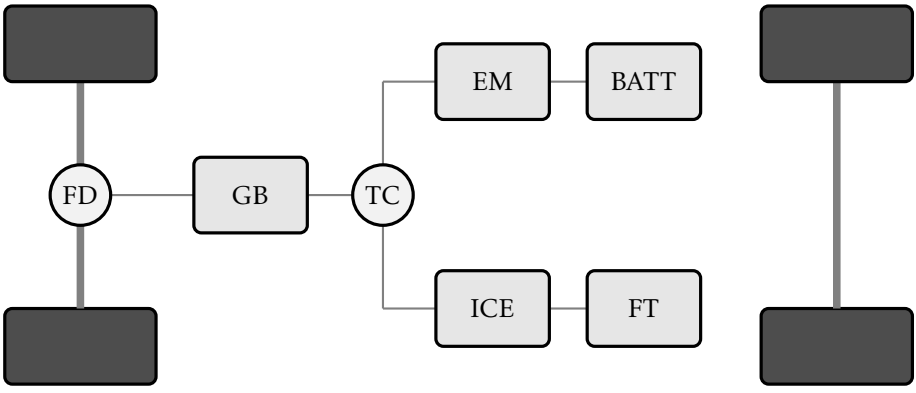

Figure 2.2: *An illustration of a parallel HEV which contains the components final drive (FD), a gearbox (GB), a torque coupler (TC), an internal combustion engine (ICE), a fuel tank (FT), an electric machine (EM), and a battery (BATT). The darker rectangles represents the wheels of the vehicle.*

2.3 Combined Hybrid

The combined hybrid is most often a parallel hybrid which contains some features from the series hybrid. It uses both a mechanical and an electric link between the engine path and the electric path and has two electric machines in addition to the combustion engine. One of the electric machines is used as a prime mover or for regenerative braking similar to a parallel HEV. The other electric machine acts like a generator, as for the series hybrid, and is used to charge the battery via the engine or for the stop-start operation [5]. Figure 2.3 shows the design of a combined HEV.

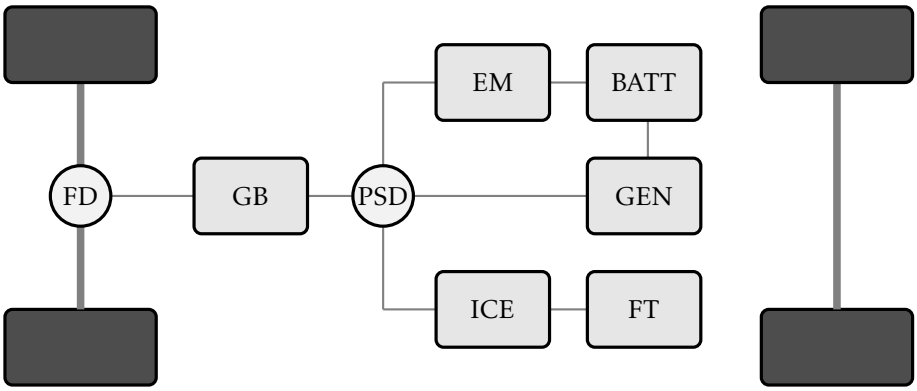

Figure 2.3: *The combined HEV contains the parts final drive (FD), a gearbox (GB), a power split device (PSD), an electric machine (EM), a battery (BATT), a generator (GEN), an combustion engine (ICE), and a fuel tank (FT). The darker rectangles represents the wheels of the vehicle.*

3

Optimization

For every HEV, a good EMS which decides how and when the two actuators (the ICE and the EM) should be engaged is necessary to achieve good fuel economy. A good way of doing this is by using optimization techniques. Depending on the application, that is if the EMS is to be implemented in a real-time controller or not, the requirements and available information differ from an EMS utilizing global optimization.

As for all optimization methods, it is important to define the optimization problem correct. The optimization problem will consist of an objective function, $J(x)$, which states what is to be maximized or minimized. A set of constraints are also defined that confines the problem, see Equation 3.1

$$\begin{aligned} &\min_{arg\ x} J(x) \\ &g(x) \leq 0 \end{aligned} \tag{3.1}$$

For an optimization problem there exist a dual problem and a primal problem, an illustration is made in Equation 3.2. If the primal problem is formulated as a minimization problem; then the dual problem is formulated as a maximization problem. [15] The optimization variables in the primal problem are referred to as primal variables (x) and for the dual problem as dual variables (y).

$$\begin{array}{llll} \textbf{Primal:} & & \textbf{Dual:} & \\ \text{minimize} & z = c^T x & \text{maximize} & v = b^T y \\ \text{subject to} & Ax \geq b & \text{subject to} & A^T y \leq c \\ & x \geq 0 & & y \leq 0 \end{array} \tag{3.2}$$

The concept of duality is an important theory in optimization. By using this theory one can guarantee optimality when the solution to the primal problem equals the solution of the dual problem and that the solution satisfies all the constraints. For Equation 3.2, it means that optimality is achieved when $z = v$ and x and y fulfill the constraints.

Another important concept derived from duality is Lagrangian duality. Lagrangian duality states that the optimization problem can be reformulated as in Equation 3.3. In the new formulation, a certain constraint can be removed if the objective function is reformulated with the Lagrangian function $L(\lambda, x)$. It can be thought of as introducing the constraint in the objective function with a cost, λ, called the Lagrangian multiplier. By choosing the variable λ properly, this penalty in the objective function can result in a very similar behaviour as if the constraint had been present. The Lagrangian multiplier for a certain constraint can be calculated by examining the dual variable for that constraint.

Primal:		**Lagrangian relaxation:**
minimize	$J(x)$	minimize $L(\lambda, x) = J(x) + \sum_{i=1}^{m} \lambda_i g_i(x)$
subject to	$g_i(x) \leq 0 \quad i = 1, ..., m$	
	$x \in X$	

(3.3)

3.1 Global Optimization

Global optimization techniques have the advantage of finding the global optimum since they use complete knowledge of the problem. The downside is that they usually are computationally heavy. When minimizing fuel consumption and NOx emissions, the objective function can be formulated as in Equation 3.4, in which the constraints can be set for the complete drive cycle. In Equation 3.4 λ_{NOx} represents a fuel equivalent factor which converts the amount of NOx emissions to equivalent fuel consumption. For a more detailed explanation of the equivalence factor see Section 3.2 or [5, 16].

$$\begin{aligned} &\min_{arg\ x} \dot{m}_f(x) + \lambda_{NOx} \cdot \dot{m}_{NOx}(x) \\ &x_{min} \leq x \leq x_{max} \end{aligned} \tag{3.4}$$

3.2 Real-time optimization

Real-time optimization techniques have the requirement of being computationally efficient. This puts constraints on the complexity of the problem which often results in having to simplify the optimization problem. The ECMS method is a popular method when implementing a real-time optimal control energy management strategy and is derived from PMP. [17]

PMP provides necessary conditions for the optimal control of a dynamical system. When PMP is applied on the energy management problem for an HEV, the state constraints are neglected and a Hamiltonian is defined that has to be minimized, see Equation 3.5.

$$H(x(t), u(t), \mu(t), t) = g(u(t), t) + \mu(t) \cdot f(x(t), u(t), t) \tag{3.5}$$

In Equation 3.5, x(t) represents the state variables, u(t) the control signals and $\mu(t)$ an adjoint state, often used in optimal control theory. Under the assumption that the internal resistance and the open circuit voltage of the battery does not depend on the state of charge, the adjoint state can be considered constant along the optimal trajectory. By introducing the costate, λ,

$$\lambda = -\mu \cdot \frac{Q_{LHV}}{U_{OC} Q_0} \tag{3.6}$$

where Q_{LHV} represents the lower heating value of the fuel, U_{OC}, the open circuit voltage of the battery, and Q_0, the battery's nominal capacity, the Hamiltonian can be rewritten as follows. [5]

$$H(t, u(t), \lambda) = P_f(w(t), u(t)) + \lambda \cdot P_{ech}(w(t), u(t)) \tag{3.7}$$

In Equation 3.7, P_f represents the fuel power and P_{ech} the electrochemical power in the battery. The costate λ acts as an equivalence factor since the fuel power and electrochemical power are not directly comparable. If λ is given a low value, then electrochemical power will be "cheaper" than fuel power resulting in depletion of the battery and vice verse. For a specific value of λ, the solution that minimizes the Hamiltonian will represent a charge sustaining trajectory for the state of charge. This is desirable when comparing different solutions.

When NOx emissions are introduced in the Hamiltonian, there will be need for a second equivalence factor. This equivalence factor will express the NOx emissions as an equivalent fuel consumption, just as λ did with the electrochemical power in the Hamiltonian stated above. [16]

3.3 Convex Optimization

One approach of implementing either a global or real time energy management strategy could be by using convex optimization. A convex optimization problem can be considered as a generalization of linear programming. The convex optimization problem has the advantage of always finding the global optimum and is often computationally efficient. It can be described for a minimization problem on the following form,

$$\begin{aligned} &\text{minimize} \quad f_0(x) \\ &\text{subject to} \quad f_i(x) \leq b_i, \ i = 1, \ldots, m. \end{aligned} \tag{3.8}$$

where the functions $f_0, \ldots, f_m$:$\mathbf{R}^n \rightarrow \mathbf{R}$ need to be convex. $x = (x_1, \ldots, x_m)$ is a vector with the optimization variables, the function f_0 is the objective function, and the functions $f_i : \mathbf{R}^n \rightarrow \mathbf{R}, i = 1, \ldots, m$ are the constraint functions with the constant limits $b_1, \ldots, b_m$. An optimal solution is obtained when the x vector has the smallest objective value among all vectors that satisfy the constraints.

In addition, in a convex optimization formulation, the constraints need to be convex or affine functions because it ensures that no local minimum exists, and the problem has only one global minimum [18].

3.3.1 Definition of convexity

The definition of a convex function is as follows. A function $f : \mathbf{R}^n \rightarrow \mathbf{R}$, where $\mathbf{R}^n$ is a generic finite-dimensional vector-space and n is its dimension, is convex if its domain f is a convex set and for all $x, y \in \text{domain} f$, and θ with $0 \leq \theta \leq 1$, the following conditions hold.

$$f(\theta x + (1 - \theta)y) \leq \theta f(x) + (1 + \theta) f(y). \tag{3.9}$$

For a first order condition, it means that if f is differentiable, meaning that ∇f exists at each value in f, then the function f is convex if and only if the domain of f is convex and

$$f(y) \leq f(x) + \nabla f(x)^T (y - x) \tag{3.10}$$

holds for all $x, y \in \text{domain} f$.

If f is a second order system and is twice differentiable, the function is convex if and only if the domain f is convex and its Hessian is positive semidefinite:

$$\nabla^2 f \succeq 0$$

Where $\succeq$ denote a generalized inequality. For vectors, it represents componentwise inequality and for symmetric matrices, it represents matrix inequality [18].

3.3.2 Embedded Conic Solver

One software package that can be used for solving convex problems is Embedded Conic Solver (ECOS), see [19]. ECOS is an interior-point solver for second-order cone programming (SOCP) designed for embedded systems. The standard form for the problem in ECOS is defined in Equation 3.11.

$$\begin{aligned} \text{minimize} \quad & c^T x \\ \text{subject to} \quad & Ax = b \\ & Gx + s \prec_K h \end{aligned} \tag{3.11}$$

The matrix G and the vector h represents the inequality constraints, where the symbol $\prec_K$ represent a generalized inequality with respect to the cone K as follows.

$$Gx \prec_K h \Leftrightarrow s = h - Gx \in K$$

and the matrix A with the vector b represents the equality constraints. The vector s represents slack variables and K the cone. x is a vector with the primal variables and c is a vector that determines and weights which variables are to be minimized.

To avoid numerical problems, it is a good idea to scale all the primal variables to values within the same short range, for example the range [-1,1]. ECOS requires the matrices A and G to be sparse matrices. Meaning that they have to be converted from full matrices into sparse form. This saves memory and is done in MATLAB with the commando *sparse*. A function call to ECOS is made with the following command:

```
[] = ecos(c',G,h,dims,Aeq,beq,opts)
```

where `dims` determines how many constraints exist, `opts` tells ECOS what options to use when solving the problem, and the rest are the matrices/vectors explained above. For more information about ECOS the reader is referred to [19].

3.3.3 Second-order cone programming

SOCP can cast problems like Matrix-fractional and Quadratically constrained quadratic programming. A brief explanation of SOCP is that it is a problem class that lies between linear or quadratic and semidefinite programming and it can be solved very efficiently by using primal-dual interior-points methods [20]. An example of a quadratic constraint is given in Equation 3.12. The second equation is written as a second-order cone and is equivalent to the first constraint equation.

$$\begin{aligned} & x^T A^T A x + b^T x + c \leq 0 \\ & \left\| \begin{matrix} (1 + b^T + c)/2 \\ Ax \end{matrix} \right\|_2 \leq (1 - b^T - c)/2 \end{aligned} \tag{3.12}$$

3.4 Model Predictive Control

The basic idea of a Model Predict Control (MPC) is to formulate the problem as an optimization problem and solve the problem on-line at each time when new measurement signals are obtained. An on-line optimization requires fast calculation time, and therefore an MPC can be a good technique.

An MPC predicts the future trajectories by using measurements from current time and control signal during each prediction horizon. If the goal is to solve a minimization problem, the objective function should be minimized while all the constraints should be satisfied. After the MPC implements the first step of the control sequence it moves the prediction horizon one step forward and repeats the optimization procedure. This is repeated for the whole drive cycle [21].

The prediction horizon is set to a specific length before running the optimization problem. A common way of choosing the length of the prediction horizon is to cover a typical settling time of the desired closed system. [22].

4

Method

In this chapter a detailed explanation is given on how the powertrain is modeled with extra focus on the fuel and NOx models. In addition, an explanation about how the optimization problem is set up using the developed models is provided. As mentioned earlier, the aim of the optimization problem defined in this thesis is to minimize NOx emissions and fuel consumption while maximizing power utilization.

4.1 Motivation

Since the requirements for a real-time EMS include both high accuracy and low computational time, it is desirable to use convex optimization techniques. Investigation of the static NOx and fuel maps obtained from steady-state measurements of the studied diesel engine shows a close-to-convex behaviour. Since the dynamic models will be an extension of the static maps, it seems reasonable to use convex optimization. However, if the convex models does not prove to be accurate enough, a different method will be used to be able to answer the questions stated in section 1.6.

4.2 Drive Cycle

To compare the performance of different vehicles, for example the amount of emissions and fuel consumption, and to ensure that legislation is enforced, standard test cycles are used. All newly-manufactured vehicles has to meet the legal requirements, and for different selling markets, there are different drive cycles that are used. The WLTC was developed to represent typical driving conditions

around the world. It is based on driving data collected around the world (EU, India, Japan, Korea, USA) combined with suitable weight factors, see [23]. The velocity profile for the WLTC drive cycle is represented in Figure A.1. One drive cycle that is used in the EPA Federal Test Procedure is the FTP-75 cycle, which was developed to measure tailpipe emissions and fuel economy of passenger cars and mimic city driving. In this thesis, both of these diving cycles are used to evaluate and compare the NOx emissions and fuel consumption. The velocity profile for the FTP75 drive cycle is presented in the appendix and is represented in Figure A.2. In addition to the WLTC and FTP75 drive cycles a random drive cycle that encapsulates city driving, in this report referred to as City drive cycle, is investigated and is presented in the appendix, see Figure A.3.

When applying global optimization techniques on the drive cycles mentioned in the paragraph above with a time step small enough to capture the engine dynamics, the computers available ran out of physical memory. Therefore segments of about 1000 seconds are evaluated for each drive cycle.

4.3 Models

In order to be able to optimize how a vehicle should use its actuators, the power request at the torque coupler should be calculated. For this purpose, a model of the powertrain, the vehicle and the speed profile is needed. In this thesis, no vehicle model is developed, instead data is collected using VSim. VSim is an in-house Simulink-based simulation tool used at Volvo Cars Corporation for analysis of the vehicles fuel economy and performance. In VSim, a mild parallel hybrid car with correct components is chosen along with a drive cycle. A simulation is made and relevant data is extracted. The data that are needed for simulation are the engine speed, w_{eng}, power request at the torque coupler, $P_{req,pt}$, the engine on/off status, eng_{on}, and the time, t.

The optimization outputs the optimal power split ratio for the torque coupler that is needed to meet the speed request from the driver/drive cycle. This power needs to be delivered by the actuators. Therefore, models for the ISG, the ICE and the battery, see Figure 2.2, need to be developed in order to set up the optimization problem.

For these components, static models are developed that only capture the steady-state behaviour. The static models for NOx emissions and fuel consumption are then expanded in order to capture the transient behaviour when going from one stationary working point to another. Since the applied optimization method is convex optimization, all of these models have to be convex.

In the remaining parts of this chapter, first the procedure of developing the models for each component that are going to be optimized is presented. Second, the dynamic fuel and NOx models are presented in detail. Finally, there is a detailed

explanation on how the convex models were developed.

4.3.1 Battery Model

The battery used in a hybrid powertrain consists of a large number of cells that are connected in series and/or in parallel. This leads to a complex electrochemical model based on partial differential equations [24], and is not suitable to be used in an energy management context. Therefore, a Thevenin equation circuit is used, see [25], which is visualized in Figure 4.1. By using this model, only the State of Charge (SoC) state is dynamic. Below, SoC is represented by ξ and is the ratio between the capacity of the battery (Q) and its nominal capacity (Q_0), see Equation 4.1.

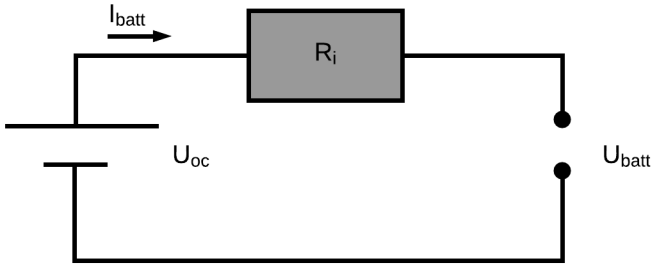

Figure 4.1: *Thevenin equivalent circuit model of a battery were U_{oc} is the open-circuit voltage, R_i is the internal resistant, I_{batt} the battery current, and U_{batt} the battery voltage.*

$$\xi(t) = \frac{Q(t)}{Q_0} \tag{4.1}$$

SoC is defined in the range $\xi \in [0,\ 1]$. To prohibit battery damage, which occurs when the battery is discharged or charged to its limits, SoC is limited by an upper bound and a lower bound. The battery open circuit voltage and inner resistance depend on the SoC. This dependency is small but still present and for the investigated battery, it has a linear behavior in the range $\xi \in [SoC_{min},\ SoC_{max}]$, see Figure 4.2. Therefore, the SoC is limited to the range $\xi \in [SoC_{min},\ SoC_{max}]$.
By combining the definition of power and Ohms law the following equations are obtained, see Equation 4.2:

$$\begin{aligned} P_{ech} &= U_{oc} \cdot I_{BATT} \\ P_{BATT} &= U_{BATT} \cdot I_{BATT} \\ P_{BATT,loss} &= U_{R_i} \cdot I_{BATT}^2 \end{aligned} \tag{4.2}$$

From these equations the power loss for the battery can be expressed as in Equation 4.3.

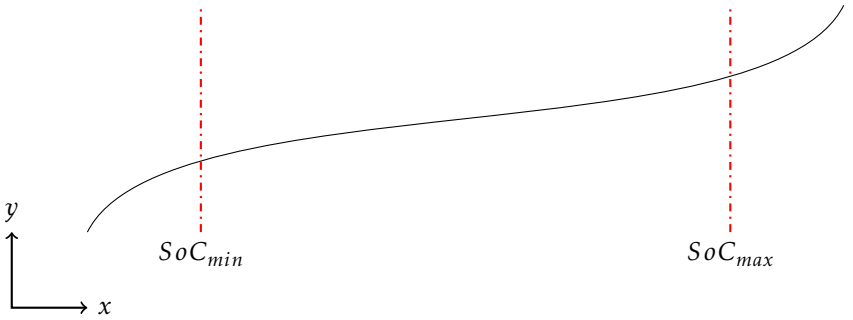

Figure 4.2: *An illustration of how the allowed values for SoC is chosen. The y-axis represent the open circuit voltage of the battery and the x-axis represent the SoC.*

$$P_{BATT,loss} = \frac{R_i}{U_{oc}^2} P_{ech}^2 \tag{4.3}$$

The inner resistance and open circuit voltage can be modeled as constants or as functions of the SoC. In this thesis Equation 4.4 is used to model both dependencies with one model, where the SoC is limited to $\xi \in [SoC_{min},\ SoC_{max}]$.

$$\frac{1}{a \cdot \xi + b} P_{ech}^2 \approx \frac{R_i}{U_{oc}^2} P_{ech}^2 \tag{4.4}$$

4.3.2 Integrated Starter Generator

For the ISG, a static power-loss map has been developed that expresses the power-loss of the component as a function of output power and rotational speed, see Equation 4.5. The static map only covers a set of stationary data points for a certain range in rotational speed and ISG output power. For values between these stationary points, linear interpolation is used and for values outside the range linear extrapolation is used based on the inclination between the last two data points in the data set. The constant γ is the ratio between engine speed and the speed of the electric machine.

$$P_{ISG,loss} = f(P_{ISG}, \omega_{ICE} \cdot \gamma) \tag{4.5}$$

The dynamics of the ISG is assumed to be small enough to be neglected.

4.3.3 Internal Combustion Engine

For the combustion engine, a static and a dynamic model for NOx emissions and fuel consumption were developed. The static models capture only the steady-state behaviour whereas the dynamic models also capture the transient behaviour.

Static Models

The static models used for both the fuel mass flow and NOx mass flow are static maps based on steady-state measurements done on the engine. These maps were developed in [13].

Fuel
The static fuel model gives a steady-state relationship between engine speed, engine output power and fuel mass flow, see Equation 4.6.

$$\dot{m}_f = f(P_{ICE,act}, \omega_{ICE}) \tag{4.6}$$

$$\dot{m}_f \cdot Q_{LHV} = P_{ICE,act} + P_{ICE,loss} \tag{4.7}$$

$$P_{ICE,loss} = f(P_{ICE,act}, \omega_{ICE}) \tag{4.8}$$

By using Equation 4.6 and Equation 4.7, a map that describes the power-losses of the engine that only covers a set of stationary points is obtained, see Equation 4.8. To extract values between these points linear interpolation/extrapolation is done as described in subsection 4.3.2.

NOx
The steady-state NOx map relates a certain NOx mass flow for a limited combinations of engine speeds and engine output powers using Equation 4.9. For engine speeds and engine torques between these stationary points the same interpolation/extrapolation method is used as described in subsection 4.3.2.

$$\dot{m}_{NOx} = f(T_{ICE,req}, \omega_{ICE}) \tag{4.9}$$

Dynamic Models

The dynamic models are an extension of the static models. To ensure that the dynamic model is convex, a dynamic part is added to the static model. If the static model and the dynamic part are convex by themselves, the sum of them will also be convex. The dynamic part is modeled so that it captures the NOx emissions/-fuel consumption when going from one stationary point to another.

Fuel

Data from [13] is used to develop the dynamic fuel model. For the positive transients, that is when going from one stationary working point to another, the difference between the actual mass flow and the mass flow given by the static fuel model ($\Delta\dot{m}_f$) is plotted as a function of the difference between the requested torque and the actual torque for different engine speeds, see Equation 4.10. The study was done for 7 different engine speeds, equally distributed.

$$\dot{m}_{f,meas} - \dot{m}_{f,stat} = f(T_{ICE,req} - T_{ICE,act}) \tag{4.10}$$

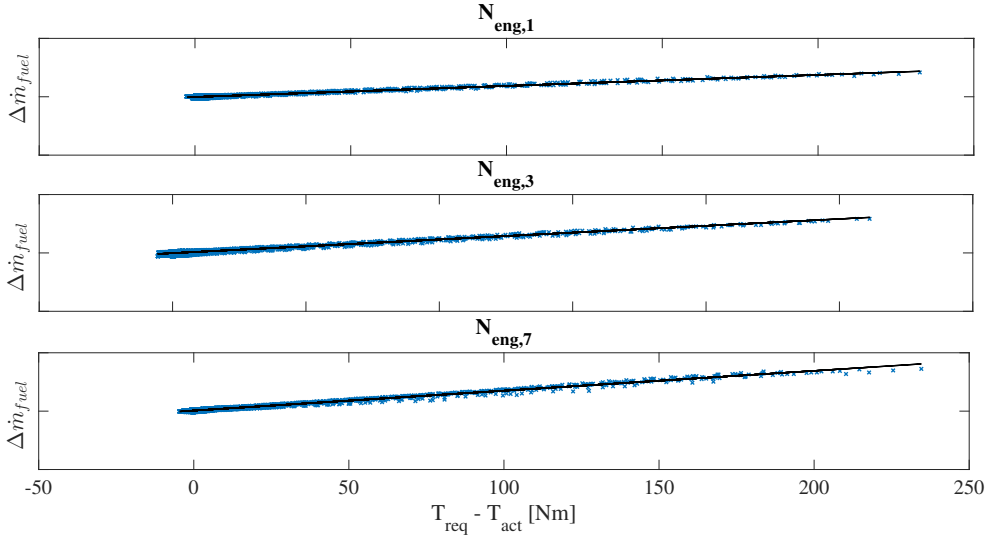

Figure 4.3: *Illustration of Equation 4.10. Blue crosses represent data points and the black line the model. Only engine speeds 1, 3 and 7 are illustrated, of the total 7 studied engine speeds.*

The relationship between $\Delta\dot{m}_f$ and $T_{ICE,req} - T_{ICE,act}$ can be approximated by a linear function for a specific engine speed, see Figure 4.3. Therefore, a simple linear model was developed using the least square method, see Equation 4.11. The variable a_k is the slope of a straight line and is a function of the engine speed ω_{ICE}. a_k is obtained for a specific engine speed using interpolation as explained in subsection 4.3.2.

$$\begin{aligned} \Delta\dot{m}_f &= a_k(\omega_{ICE}) \cdot (T_{ICE,req} - T_{ICE,act}) \\ \dot{m}_{f,dyn} &= \dot{m}_{f,stat} + \Delta\dot{m}_f \end{aligned} \tag{4.11}$$

NOx

The same approach used for the dynamic fuel model was used for the dynamic NOx model. However the NOx peaks have an offset in time to when the torque step is made, see Figure 4.4. This offset is not constant and is probably caused by sensor dynamics and efforts of compensating for this offset. Most likely it does not represent the actual relationship between a transient engine operation and the resulting NOx emissions. As explained in [2, 3, 11–13] and Section 1.3.2, a transient engine operation occurs due to a change in engine speed or engine load. This in turn causes a disturbance in the combustion chamber and the air entrapment until steady-state engine operation is attained. Since NOx formation is highly dependent on the temperature in the engine cylinders which during an engine transient will increase, it may lead to a NOx peak. Therefore, it is reasonable to assume that the delay is caused by sensor dynamics and the NOx peak occurrs at the same time as the torque step.

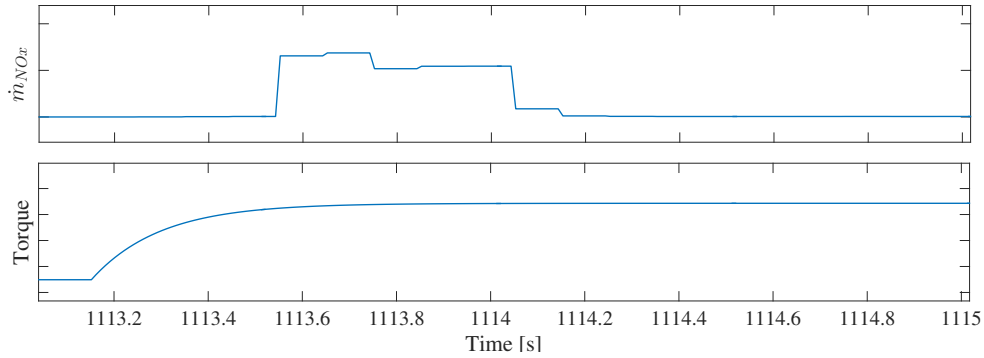

Figure 4.4: *Illustration of the offset in time between a torque step and the NOx peak.*

To find a relationship between the torque step and the additional NOx emissions resulting from this torque step, several approaches were tested. The approach closest to have a reasonable relationship was Equation 4.12.

$$\Delta NOx = \ln\left(\int_{t=t_{trans,start}}^{t=t_{trans,end}} \frac{NOx_{meas} - NOx_{stat}}{0.9t} dt\right) = f(T_{ICE,req} - T_{ICE,act}) \quad (4.12)$$

Figure 4.5 shows ΔNOx as a function of $T_{req} - T_{act}$ defined in Equation 4.12.

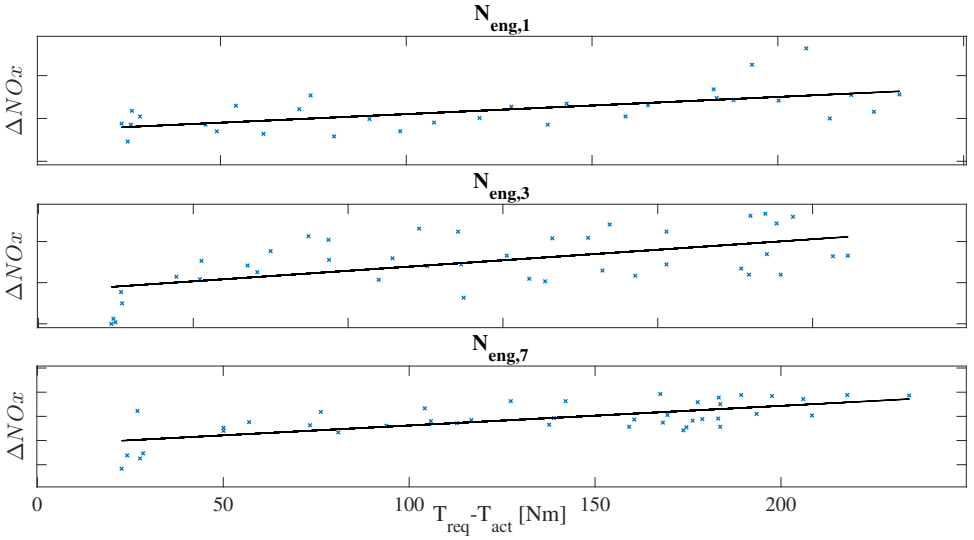

Figure 4.5: *Illustration of Equation 4.12 where the blue crosses represents data and the black line is the model. Only engine speeds 1,3 and 7 are illustrated, out of the 7 studied engine speeds.*

When ΔNOx was added to the static model and compared to the measured values, the dynamic model (static NOx plus ΔNOx) did not behave as the measurements did. Therefore, a different dynamic NOx model had to be found.

Another NOx model that was evaluated was inspired by [2], see following Equation 4.13.

$$\begin{aligned} \dot{m}_{NOx,dyn} &= \dot{m}_{NOx,stat} \cdot (1 + c \cdot \frac{T_{ICE,act}(t_k) - T_{ICE,act}(t_{k-1})}{T_s}) \\ c &= \frac{m_{NO_x,tot} - \sum_{k=1}^{N} \dot{m}_{NO_{x,stat}}(t_k) \cdot T_s}{\sum_{k=1}^{N} \dot{m}_{NO_x,stat}(t_k) \cdot T_s \cdot max(\frac{T_{ICE,act}(t_k) - T_{ICE,act}(t_{k-1})}{\Delta t}, 0)} \end{aligned} \tag{4.13}$$

In Equation 4.13, the index tot refers to the cumulative sum of measurements made for the complete drive cycle that the model is made for, i.e. the model in [2] is cycle dependent. The index $stat$ represent values interpolated from a steady-state engine map, and T_s is the sampling time.

However, the model developed in [2] is not convex and would have to be modified to be used in convex optimization method. This was attempted and evaluated without obtaining a good model.

A quadratic NOx model, see Equation 4.14, was also investigated but with no success. It gives positive NOx mass flows at negative transients, because the constant $B_{quad,NOx}$ could not be tuned in a way which would compensate for the positive contribution that is made by the first quadratic term containing the constant $A_{quad,NOx}$.

$$\begin{aligned} \dot{m}_{NOx,dyn} &= \dot{m}_{NOx,stat} + A_{quad,NOx} \cdot \Delta T^2 - B_{quad,NOx} \cdot \Delta T \\ \Delta T &= T_{ICE,req} - T_{ICE,act} \end{aligned} \tag{4.14}$$

The model used in this thesis, see Equation 4.15, is a linear model based on the characteristics seen in Figure 4.5 as well as it being physically reasonable. The model is fitted using the cumulative sum of the measurements from [13] by tuning the constant A_{NOx}. The variable ΔT is the same variable used in Equation 4.14.

$$\dot{m}_{NOx,dyn} = \dot{m}_{NOx,stat} + A_{NOx} \cdot \Delta T \tag{4.15}$$

Validation of the models used is found in chapter 5 and chapter 6.

Engine Torque

Since the purpose of this thesis is to evaluate the impact of engine dynamics, a model that captures the major dynamics of the engine is needed. The dominating dynamics for the engine is caused by the turbo lag which causes the engine torque to lag behind the requested torque. By investigating measurement data of the engine torque obtained from [13], a model is developed and fitted. The torque behaves like a first order system and is modeled using Equation 4.16 where the time constant τ need to be determined. This is done by analyzing the characteristics of the torque steps.

$$T_{ICE,act}(t+1) = T_{ICE,act}(t) + \frac{T_{ICE,req(t)} - T_{ICE,act}(t)}{\tau} \Delta t \tag{4.16}$$

4.3.4 Convex Models

In order to be able to construct a convex optimization problem, the objective function and the constraints need to be convex or concave, see section 3.3. Note that since the velocity profile of the car as well as the selected gear is considered to be known the engine speed can be calculated. Therefore, the models for each component need only depend on the output power in a convex/concave order, depending on if something is minimized/maximized.

The dynamic extension that is added to the static models for NOx emissions and fuel consumption are convex. However, the static maps for each component except for the battery are not convex. The battery losses can be expressed as in Equation 4.17 which is a convex expression. a_{SoC} represents the inclination and b_{SoC} the offset for the relationship between the U_{OC} and the SoC.

$$P_{BATT,loss} = \frac{R_i}{U_{oc}(\xi)^2} P_{ech}^2 = \frac{P_{ech}^2}{a_{SoC} \cdot \xi + b_{SoC}} \tag{4.17}$$

The static maps for the NOx mass flow, the power-losses for the ICE and the power-losses for the ISG indicate a close to convex behaviour which is one of the reasons convex optimization was chosen. The procedure of making these static models convex is done through piecewise linearization.

Piecewice Linearization

Piecewise linearization is illustrated in Figure 4.6 and it is applied on the static maps listed above. To ease understanding, we consider the power loss model for the ICE but the concept is exactly the same for the other static maps. For a set of predefined engine speeds, the power losses are approximated with a number of straight lines whose slopes are increasing with increasing output power, $P_{ICE,act}$. By taking the maximum value of all straight lines for a specific output power, a value close to that of the non convex model is obtained. Considering Figure 4.6, y and x can represent $P_{ICE,loss}$ and $P_{ICE,act}$ respectively and this would be for one specific engine speed. The number of lines for each engine speed is a design variable and the process is repeated for a predefined number of engine speeds until a sufficiently correct convex map is obtained. In order to extract information from the map for a engine speed that is not explicitly defined in the convex maps, the same interpolation/extrapolation method as explained in subsection 4.3.2 is used.

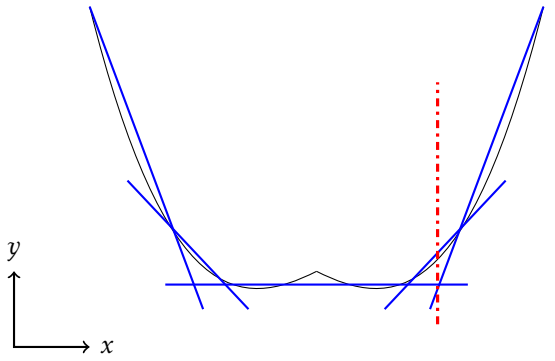

Figure 4.6: *An illustration of piecewise linearization.*

4.4 Optimization

By using the models developed in section 4.3, the optimization problem is constructed. The aim of the optimization is to minimize fuel consumption and NOx emissions while maximizing power utilization by optimizing the torque split. The optimization problem will be formulated as a global optimization problem as well as a real-time optimization problem using MPC and ECMS. These two optimization strategies will then be divided into to subsets, one only utilizes convex static models and the other one uses convex dynamic models, see Figure 4.7. The optimal torque split for the different optimization methods and the effect that it has on NOx emissions and fuel consumption will then be evaluated using two different plants.

The two plants are referred to as *Plant 1* and *Plant 2*. Plant 1 is in this thesis represented by the convex dynamic models constructed in this thesis. Plant 2 is represented by the non-convex static maps with the same dynamics used in Plant 1, that is the convex dynamic extension for both fuel and NOx. The fuel model used in Plant 2 is described by Equation 4.11 where $\dot{m}_{f,stat}$ is the non-convex static fuel map. The NOx model used in Plant 2 is represented in Equation 4.15 where $\dot{m}_{NOx,stat}$ refers to the non-convex static NOx map.

By analyzing the results obtained from Plant 1, an answer to the questions stated in section 1.6 is obtained under the assumption that the controller has perfect models describing the plant. The results obtained when using Plant 2 will instead answer the same questions but for the scenario when the controller does not have perfect models describing the plant.

Since no driver model is constructed, the modeled torque is implemented in the static optimization where the requested torque represents the driver and the actual torque are the output from the engine. This is a reasonable simplification that can answer the questions in section 1.6.

In order to be able to compare the different methods, the solution obtained from the optimization needs to be charge sustaining. It means that the final value for the battery SoC has to be the same (within reasonable tolerances) as the start value of the SoC.

The software package used for setting up the optimization problem is ECOS. To implement the MPC, ECOS will be used since it is suitable for a real-time controller.

For simplicity of notations, all variables are expressed in terms of power. The equivalent power of a certain fuel mass flow is calculated by using Equation 4.18 where Q_{LHV} is the lower heating value for diesel. The NOx mass flow equivalent power is calculated the same way but is not a physical quantity and should be thought of as a scaled up NOx mass flow.

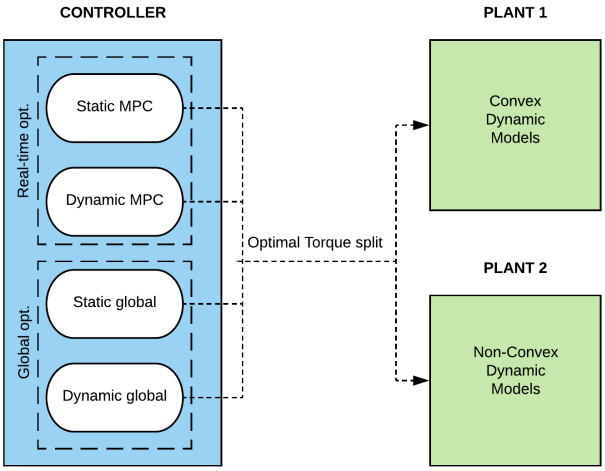

Figure 4.7: *Illustration of the controller, where the different EMS are implemented, and the two plants used in this thesis.*

$$\begin{aligned} P_f &= m_f \cdot q_{LHV} \\ P_{NOx} &= m_{NOx} \cdot q_{LHV} \end{aligned} \tag{4.18}$$

In the next section, a description is given on how the global and real-time (MPC) optimization problems are constructed followed by an explanation on how they are implemented in ECOS.

Convexity

In subsection 4.3.4, the approach that was used when the convex models were developed is explained. There exist limits on the maximum and minimum power for the different components which are given as 1 dimensional look up tables. However, they only are dependent on the rotational speed which is given and therefore, are a known constant in each time step. Hence, they do not need to be convex but are still modeled using piecewise linearization and the given 1 dimensional look up tables. For the battery, the maximum and minimum limits are constant values that are independent of time.

Equivalence Factors

There are two equivalence factors that are used in this thesis, λ_{NOx} and λ_{ech}. λ_{NOx} was obtained by one of our supervisors at Volvo Cars Corporation by calculating the equivalent fuel consumed (using engine measures such as the EGR and fuel timing) for reducing NOx emissions. It weights one gram of NOx equal to one gram of fuel. λ_{ech} is derived using theory briefly explained in chapter 3. It is obtained by solving the global optimization problem stated below and extracting the dual variable correlated to the following Equation 4.19.

$$P_{ech}(t) = \frac{SoC(t) - SoC(t+1)}{dt} \cdot Q_0 \cdot U_{OC} \tag{4.19}$$

The equivalence factor λ_{ech} is further explained in subsection 4.4.2.

Convex relaxation

When implementing the convex models that were created with piecewise linearization, a convex relaxation has to be made since the max-function does not necessarily have a continuous first order derivative. Instead, if using the example in section 4.3.4 where the max-function is used in the same way as below, a convex relaxation is made as in Equation 4.21.

$$P_{ICE,loss} = \max(a_1 \cdot P_{ice,act} + b_1, a_2 \cdot P_{ice,act} + b_2, \ldots, a_n \cdot P_{ice,act} + b_n) \tag{4.20}$$

In the rest of this section, Equation 4.20 is substituted with the convex relaxation in Equation 4.21, that can be implemented for convex optimization problems. As long as $P_{ICE,loss}$ or a variable that depend on it is being minimized the model approximation will be valid.

$$\begin{aligned} P_{ICE,loss} &\geq a_1 \cdot P_{ICE,act} + b_1 \\ P_{ICE,loss} &\geq a_2 \cdot P_{ICE,act} + b_2 \\ &\vdots \\ P_{ICE,loss} &\geq a_n \cdot P_{ICE,act} + b_n \end{aligned} \tag{4.21}$$

In the Equations above, n represents the number of lines used when approximating a function with a piecewise linear function, and the a:s and b:s represents the inclinations and offsets of the lines. This relaxation is made for all losses, i.e. for the battery, the ISG and the ICE as well as for the NOx emissions.

4.4.1 Global Optimization

The global optimization has the objective of determining the optimal torque split that minimizes fuel consumption and NOx emissions. It uses complete knowledge of the drive cycle and the optimization problem is formulated as below. First, the static global optimization problem is defined followed by the dynamic global optimization problem.

Static Optimization

The objective function for the static optimization is defined as in Equation 4.22.

$$\begin{aligned}[P_{ICE,act}\ P_{ISG}] =& \text{argmin } J \\ J =& dt \cdot [P_{f,stat}(P_{ICE,act})] + \\ & dt \cdot \lambda_{NO_x} \cdot [P_{NOx,stat}(P_{ICE,act})]\end{aligned} \tag{4.22}$$

In Equation 4.23 and Equation 4.24 the equality and inequality constraints that define the static optimization problem are represented where U_{oc} and Q_0 represent the open circuit voltage and the nominal capacity respectively. The constants a and b for the ICE, NOx and ISG are the slopes and offsets for the straight lines constructed when creating the convex static maps using piecewise linearization, see section 4.3.4.

Note that the sum of the produced torque from the ICE and ISG (P_{ICE}, P_{ISG}) is allowed to be greater than the requested torque (P_{req}). If the optimization is done correct, this will only occur for negative torques which cannot be supplied by the two actuators. This means that the driver would need to apply the vehicle friction brakes in order to achieve the requested torque.

Equalities:

$$\begin{aligned} P_{ech}(t) &= \frac{SoC(t) - SoC(t+1)}{dt} \cdot Q_0 \cdot U_{OC} \\ P_{ech}(t) &= P_{BATT,loss} + P_{ISG,act} + P_{ISG,loss} + P_{aux} \\ P_{ICE}(t+1) &= [P_{ICE}(t) + \frac{P_{ICE,req}(t) - P_{ICE}(t)}{\tau} \cdot dt] \cdot \frac{\omega_{ICE}(t+1)}{\omega_{ICE}(t)} \\ SoC(t=1) &= SoC_{start} \end{aligned} \tag{4.23}$$

Inequalities:

ISG equations:

$$\begin{aligned} &P_{ISG,loss}(t) \geq 0 \\ &P_{ISG}(t) \geq P_{ISG,min}(t) \\ &P_{ISG}(t) \leq P_{ISG,max}(t) \\ &P_{ISG,loss}(t) \geq a_{ISG}(\omega_{ISG}) \cdot P_{ISG}(t) + b_{ISG}(\omega_{ISG}) \end{aligned}$$

ICE equations:

$$\begin{aligned} &P_{ICE,loss}(t) \geq a_{ICE}(\omega_{ICE}) \cdot P_{ICE,act}(t) + b_{ICE}(\omega_{ICE}) \\ &P_{ICE,act}(t) \geq P_{ICE,min}(t) \\ &P_{ICE,act}(t) \leq P_{ICE,max}(t) \\ &P_f(t) \geq 0 \\ &P_{ICE,loss}(t) \geq 0 \\ &P_f(t) \geq P_{ICE,act}(t) + P_{ICE,loss}(t) \\ &P_{req}(t) \leq P_{ICE,act}(t) + P_{ISG}(t) \end{aligned}$$

NOx equations:

$$\begin{aligned} &P_{NOx}(t) \geq a_{NOx}(\omega_{ICE}) \cdot P_{ICE}(t) \cdot q_{LHV} + b_{NOx}(\omega_{ICE}) \cdot q_{LHV} \\ &P_{NOx} \geq 0 \end{aligned}$$

Battery equations:

$$\begin{aligned} &P_{BATT,max} \geq P_{ISG}(t) + P_{ISG,loss}(t) + P_{aux} \\ &P_{BATT,min} \leq P_{ISG}(t) + P_{ISG,loss}(t) + P_{aux} \\ &SoC(t) \leq SoC_{max} \\ &SoC(t) \geq SoC_{min} \\ &SoC(t = t_{end}) \geq SoC_{start} \\ &P_{BATT,loss} \geq \frac{P_{ech}^2}{a_{SoC} \cdot SoC(t) + b_{SoC}} \end{aligned} \tag{4.24}$$

Dynamic Optimization

The objective function for the dynamic global optimization is defined in Equation 4.25.

$$\begin{aligned}[P_{ICE,req}\ P_{ISG}] &= \text{argmin } J \\ J &= dt \cdot [P_{f,stat}(P_{ICE,act}) + P_{f,dyn}(P_{ICE,act}, P_{ICE,req})] \\ &\quad + dt \cdot \lambda_{NO_x} \cdot [P_{NOx,stat}(P_{ICE,act}) \\ &\quad + P_{NOx,dyn}(P_{ICE,act}, P_{ICE,req})]\end{aligned} \tag{4.25}$$

The indexes req and act refer to the requested power and the actual output power of the actuator respectively. These powers will be different for the ICE due to the dynamics, but for the ISG the power will be equal since the dynamics are neglected in the optimization.

Equation 4.26 and Equation 4.27 are added to the static problem defined by Equation 4.23 and Equation 4.24 to reflect the dynamics of the system. The constraint on the power of the fuel, P_f, in Equation 4.24 ($P_f(t) \geq P_{ICE,act}(t) + P_{ICE,loss}(t)$) is replaced by: $P_f(t) \geq P_{ICE,act}(t) + P_{ICE,loss}(t) + P_{ICE,dyn}(t)$, represented in Equation 4.27.

Equalities:

$$\Delta T(t) = \frac{P_{ICE,req}(t) - P_{ICE,act}(t)}{\omega_{ICE}(t)} \tag{4.26}$$

Inequalities:

$$\begin{aligned}P_{ICE,dyn}(t) &\geq \frac{a_k(\omega_{ICE}) \cdot (P_{ICE,req}(t) - P_{ICE,act}(t))}{\omega_{ICE}(t)} \\ P_{ICE,dyn}(t) &\geq 0 \\ P_f(t) &\geq P_{ICE,act}(t) + P_{ICE,loss}(t) + P_{ICE,dyn}(t) \\ P_{NOx,dyn}(t) &\geq A_{NOx} \cdot \Delta T(t) \cdot q_{LHV} \\ P_{NOx,dyn}(t) &\geq 0\end{aligned} \tag{4.27}$$

The factor τ is the time constant for the torque dynamics of the ICE and a_k is a speed dependent inclination for the linear model capturing the extra fuel consumption due to transient engine operation.

4.4.2 Real-Time Optimization

The purpose of the real-time optimization strategy is to find the optimal torque split that minimizes both fuel consumption and NOx emissions. Unlike the global optimization strategy, the MPC in this thesis does not utilize complete knowledge of the drive cycle. Instead it has limited look ahead knowledge defined by a predefined prediction horizon. The solutions obtained from the MPC and the global optimization are set to be charge sustaining in order to to make a fair comparison between the different methods. The ECMS approach is applied and a Hamiltonian is introduced and minimized by finding the optimal torque split. The Hamiltonian is defined in a different way for the static and dynamic optimization. An illustration of the MPC is represented in Figure 4.8.

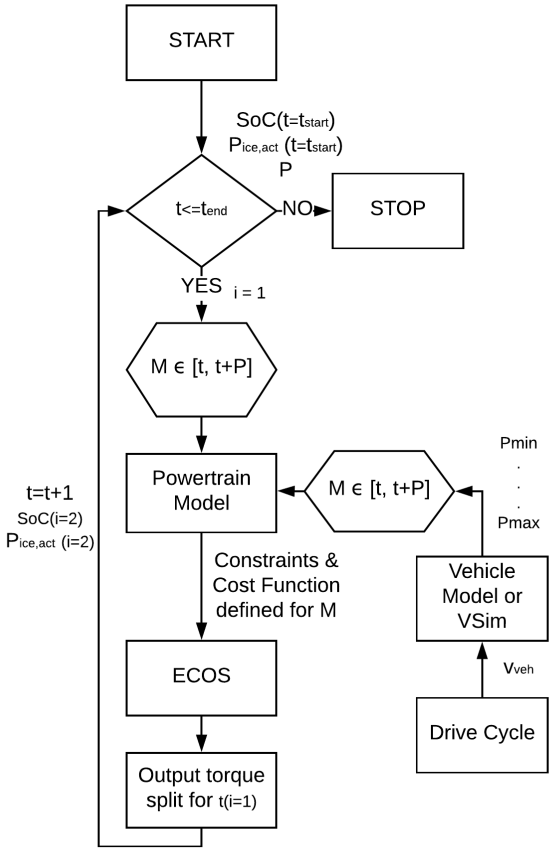

Figure 4.8: *Flowchart for the MPC. The subproblem M defines the problem that the MPC solves for each iteration.*

Static Optimization

The Hamiltonian that is to be minimized using the static MPC is defined as follows.

$$H = \sum_{i=1}^{k} P_{f,stat}(P^i_{ICE,act}) + \lambda_{NO_x} \cdot P_{NOx,stat}(P^i_{ICE,act}) + \lambda_{ech} \cdot P_{ech}(P^i_{ISG}, SoC^i) \tag{4.28}$$

where k is the prediction horizon. The optimization problem for the static MPC is then defined in Equation 4.29.

$$[P_{ICE,act}\ P_{ISG,act}] = \text{argmin}\ dt \cdot H \tag{4.29}$$

The same equations stated in Equation 4.23 and Equation 4.24 are used except for the constraint $SoC(t = end) \geq SoC_{start}$. The equivalence factor λ_{ech} multiplied with P_{ech} is instead added to the cost function. By tuning λ_{ech} correctly, a charge sustaining trajectory is obtained.

Dynamic Optimization

The Hamiltonian that is to be minimized in the dynamic optimization is represented in Equation 4.30 and the optimization problem for the dynamic MPC is defined in Equation 4.31.

$$\begin{aligned} H = & \sum_{i=1}^{k} P_{f,stat}(P^i_{ICE,act}) + P_{f,dyn}(P^i_{ICE,act}, P^i_{ICE,req}) \\ & + \lambda_{NO_x} \cdot [P_{NOx,stat}(P^i_{ICE,act}) + P_{NOx,dyn}(P^i_{ICE,act}, P^i_{ICE,req})] \\ & + \lambda_{ech} \cdot P_{ech}(P^i_{ISG}, SoC^i) \end{aligned} \tag{4.30}$$

$$[P_{ICE,req}\ P_{ICE,act}] = \text{argmin}\ dt \cdot H \tag{4.31}$$

The equalities and inequalities stated in Equation 4.26 and Equation 4.27 are used for the MPC as well except for the terminal constraint on the SoC, that is $SoC(t = end) \geq SoC_{start}$. Similar to the static MPC, the term $\lambda_{ech} \cdot P_{ech}$ is instead added to the cost function.

4.4.3 Embedded Conic solver

ECOS uses matrices to solve the optimization problem in which all the constraints are formulated in matrix form. The optimization is time dependent where different equations are needed for different time steps. Therefore, the matrices G and A are constructed for every time step and then placed in separate higher dimensional matrices. They are placed in the diagonal of the new matrices. This makes it possible to use previous values in an efficient way by having the smaller matrices for different time steps overlap each other in the higher dimensional matrix

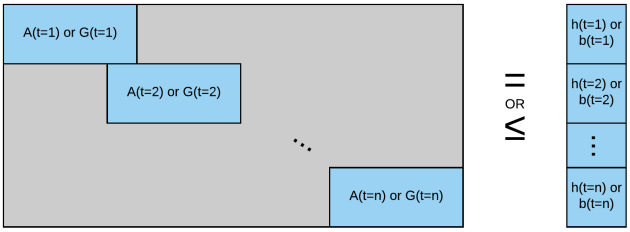

Figure 4.9: *Illustration of how the matrices are placed diagonal after each other for every time step, in order to create one higher dimensional matrix. The lighter gray represents zeros and each blue rectangle represents a matrix for one time step. Here n time steps are assumed. The equality is used for A and b, see Equation 4.32, and the inequality is used for G and h, see Equation 4.33.*

as illustrated in Figure 4.9. Parameters b, h, and c are row vectors and not matrices so they are placed after each other for every time step. c is not illustrated in Figure 4.9 but is the vector defining the cost vector and the same logic applies for c as for b and h.

Second order cone

The quadratic constraint in Equation 4.24 has to be implemented in ECOS as a second-order cone, see Equation 3.12. The conversion from a quadratic constraint to a SOCP is done by using the python toolbox Quadratic Cone Modeling Toolbox (QCML), see [26].

Scaling

As mentioned in subsection 3.3.2, scaling factors are needed in order to avoid numerical problems. A specific scaling factor, α, is derived for every variable and a specific scaling factor β is derived for every equation. The scaling factor α scales the variables to be in the same value range and as a result numerical problems can be avoided. The variable β scales the equations and is used to make the solver find a solution faster by prioritizing certain equations. For a better understanding of how the scaling is made, see Equations (4.32) – (4.34).

$$\frac{A\alpha}{\beta}x = \frac{b}{\beta} \qquad (4.32) \qquad\qquad \frac{G\alpha}{\beta}x \leq \frac{h}{\beta} \qquad (4.33)$$

$$c^T \cdot \alpha \qquad (4.34)$$

5
Validation

The validation is divided into two main parts. The first part is model validation, which is important to answer the first question posed in this thesis, see section 1.6.

– *Is it possible to save fuel and reduce NOx emissions by considering dynamic actuator behaviour when developing an optimal EMS for a charge sustaining HEV?*

To be able to answer the question stated above, a comparison is made on how the solution obtained from the controller using the dynamic models differs from the solution obtained from the controller using only the static models. This comparison is made for both the global optimization and the MPC using both Plant 1 and Plant 2.

To answer the second question posed in this thesis,

– *By using a prediction horizon, is it possible to save fuel and reduce NOx emissions, and how does the length of the prediction horizon affect the emissions and fuel consumption?*

the solutions obtained from the MPC with different prediction horizons are investigated to find the most suitable prediction horizon for the static model and the dynamic model. To isolate the effect of engine dynamics, an iterative bisection algorithm is developed that find the equivalence factor, λ_{ech}, that results in a charge sustaining optimal solution. The algorithm is applied on each drive cycle for a set of different prediction horizons. All three drive cycles are investigated for both static and dynamic models.

5.1 Models

The validation variables that have been used here are RMSE, error of variance, and errors of cumulative sums. The RMSE is the mean of the relative error between the evaluated model and the measured value at each sample time.

Since there is a varying offset in time between the torque step and the corresponding NOx peak, see Figure 4.4, the RMSE cannot be used since there is no way to know where the NOx peak should be if no sensor delays, compensation of these delays, etc would have been present. Therefore, an error of variance is used to get measurable values on how well the models capture transient behavior. This is done by taking the difference between the model and a reference signal that has the shape of a square wave. The reference signal represents a completely static behaviour with instantaneous change in value when going from one static point to another one. Then, the variance is calculated for the difference between the model and the reference signal. This value gives an indication on how well a model captures the transient behaviour when compared to the variance for the difference between the actual values (measurements) and the reference signal. The error of variance is then expressed as the relative error between the variance for the reference signal subtracted from the model and the reference signal subtracted from the measured values, where the latter represents the correct value of the variance.

The error of cumulative sum is also expressed as a relative error, where the cumulative sum of the measured signal represents the correct value.
The developed models for fuel and NOx are validated using data from measurements produced in [13] for both Plant 1 and 2. In Table 6.2 and Table 6.6, Plant 1 is referred to as the *Convex Model* and Plant 2 is referred to as the *Non-Convex Static Model*.

When validating the different optimization methods, the two different plants are used as illustrated in Figure 4.8 and explained in section 4.4.

5.1.1 Torque

In order to get an accurate and exact validation, all models are validated with the modeled torque; therefore, the torque is validated first. As mentioned before the torque model is a first order system fitted to measurement data produced in [13], and therefore, it is validated against the measured data.

Validation of the torque model is done using RMSE and the error between the cumulative sums, and also, with a figure to visualize the comparison between the modeled and measured torques. The cumulative sum is always calculated using the same length of the same drive cycle.

5.1.2 Fuel

Since the convex static fuel models are an approximation of static models, they are validated against each other. But also, in order to get a better understanding of how the convex static fuel maps match reality, they are validated against measurement data [13]. An illustration for two torque steps is made with all the models to visualize how they relate to each other.

5.1.3 NOx

The same validation method as for fuel is used for NOx, and the convex static maps are validated against both static maps and measured data. The errors are represented in Tables 6.6 and 6.7 and the different models are illustrated in Figures 6.3 to 6.6 that are presented in chapter 6.

5.2 Optimization

In this section, the results obtained from the different optimization techniques are presented. First, the torque trajectories for the ISG and ICE are shown for the solution obtained from both the global optimization and the MPC, using both static and dynamic models, in order to emphasize the difference between the solutions when considering engine dynamics. Thereafter, the cost function is evaluated for each drive cycle and several prediction horizons including the global solution using both the static and dynamic models. These results are presented both as figures in chapter 6 and in a table in Appendix B.

The SoC trajectory is also investigated for each drive cycle, both for the static and the dynamic controller, and are presented in in figures in chapter 6.

Another variable of interest is the calculation time for the MPC and how it changes when using different prediction horizons. Therefore, an illustration of the correlation between the length of the prediction horizon and the computational time is made in figures presented in chapter 6.

6
Results

In this chapter, all the results are presented and for more explanation of what is presented read associated sections in chapter 5. The sections in this chapter are the same as in chapter 5 to simplify for the reader how a specific result was obtained. The developed models are presented first and thereafter the optimization method will be described.

6.1 Models

In this section, the results for the torque, fuel, and NOx models are presented.

6.1.1 Torque

For the torque model, the calculated error between the model and measurements are presented in Table 6.1. How the model fits the measured torque is illustrated in Figure 6.1. The Cumulative sum error is very small and the RMSE is relatively small. The relative error becomes very large for engine torques close to and below zero. For larger absolute values of the engine torque the relative error is a lot smaller.

Table 6.1: *Validation of the torque model, using measured torque values.*

Torque	**RMSE [%]**
Modeled Torque vs measured torque	10.79
	Cumulative Sum Eorror [%]
Modeled Torque	0.21

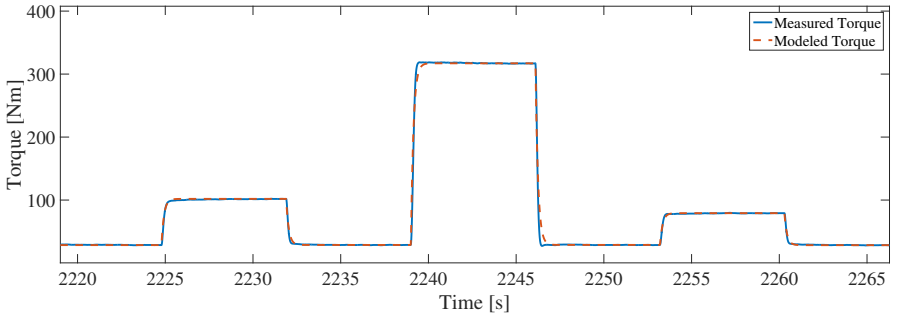

Figure 6.1: *An illustration of the modelled torque together with the measured torque.*

6.1.2 Fuel

The result of the static and the dynamic fuel model are presented in Tables 6.2 to 6.5 and Figure 6.2.
The convex static fuel model has a larger relative error than the static non-convex model when compared to the measured values, see Table 6.2. It can be seen in Figure 6.2 that the convex approximation often overestimates the static non-convex model and this overestimation is approximately the same in value for low values of fuel consumption and high values of fuel consumption, resulting in a high relative error for low values of fuel consumption. This is a consequence from that the convex approximation is especially bad for low and negative engine torques. A consequence from this is that the convex dynamic model also performs bad for low and negative torques.

Interesting to notice is that if the dynamic model is added to the non-convex static model, a much lower RMSE value is obtained, see Tables 6.2 and 6.3.

In addition, the same errors were calculated for torques above 15 newton meters (Nm) and these are presented in Table 6.4. These values show that for torques above 15 Nm the convex approximation is not as bad which in turn results in a better convex dynamic model.

Table 6.2: *Validation of the static fuel models.*

Static Fuel	**Cumulative Sum Error [%]**
Non-Convex Model vs Measurements	0.0022
Convex Model vs Measurements	5.42
Convex Model vs Non-convex Model	5.23
	RMSE [%]
Non-convex Model vs Measurements	4.83
Convex Model vs Measurements	11.00

Table 6.3: *Validation of the dynamic fuel model.*

Dynamic Fuel	**Cumulative Sum Error [%]**
Convex Model vs Measurements	5.43
	RMSE [%]
Convex Model vs Measurement	8.58
Non-convex Model vs Measurement	2.28

Table 6.4: *Validation of the static fuel models, using data for engine torques above 15 Nm.*

Static Fuel	**RMSE [%]**
Non-convex Model vs Measurements	5.75
Convex Model vs Measurements	9.77

Table 6.5: *Validation of the dynamic fuel model, using data for engine torques above 15 Nm.*

Dynamic Fuel	**RMSE [%]**
Convex Dynamic Model vs Measurements	5.37
Non-convex Dynamic Model vs Measurements	2.66

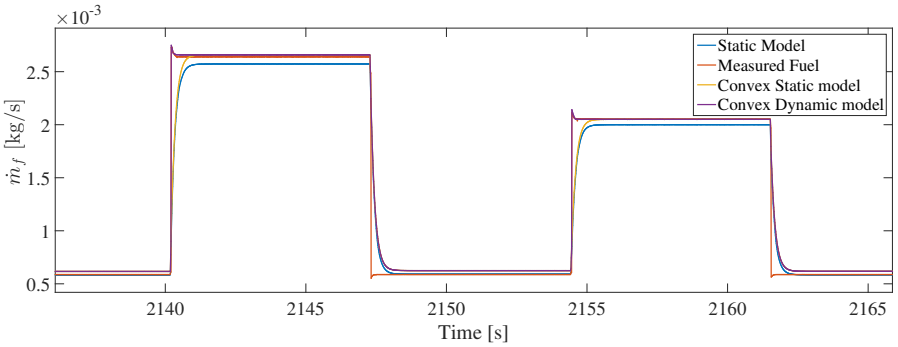

Figure 6.2: *All fuel models in the same figure to illustrate how they relate to each other. The behaviour of the fuel mass flow is a consequence of torque steps made for the engine.*

6.1.3 NOx

In this subsection, the results of the static and the dynamic NOx models are presented. The difference between the convex static model and the static non-convex model is larger for NOx than for fuel. The convex NOx model also overestimates

the NOx consumption and the approximation is worse for low and negative engine torques. The improvement by only considering engine torques above 15 Nm is better for NOx than for fuel.

Table 6.6: *Validation of the static NOx models.*

Static NOx	**Cumulative Sum Error[%]**
Non-convex Model vs Measurements	77.29
Convex Model vs Measurements	77.54
Non-convex Model vs Convex Model	1.15
	Variance Error [%]
Non-convex Model vs Measurements	0.0383
Convex Model vs Measurements	0.0355
	RMSE [%]
Convex Model vs Non-convex Model	29.18
Convex Model vs Non-convex Model (T_{ICE} above 15Nm)	18.85

Table 6.7: *Validation of the dynamic NOx model.*

Dynamic NOx	**Cumulative Sum Error [%]**
Measurements vs Convex Model	$2.05 \cdot 10^{-6}$

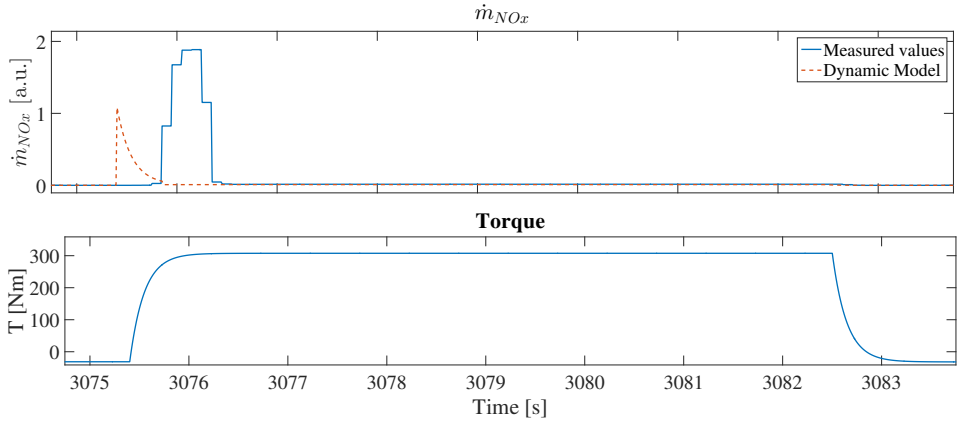

Figure 6.3: *Dynamic NOx model together with measured NOx values where the dynamic NOx is smaller than the measured value.*

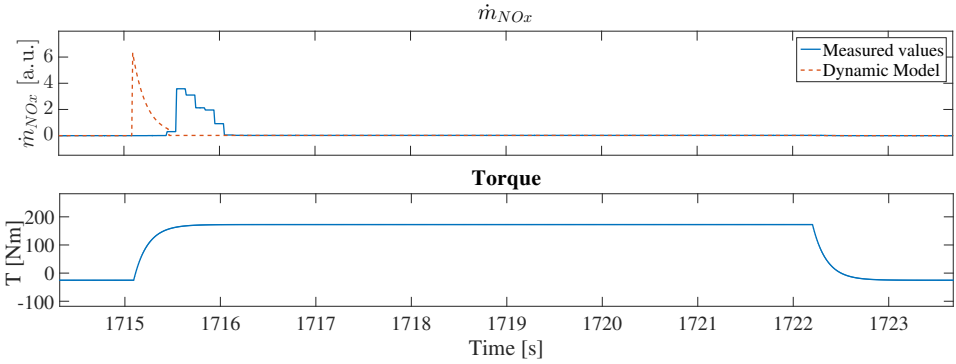

Figure 6.4: *Dynamic NOx model together with measured NOx where the dynamic NOx is higher than the measured values.*

By looking at Figure 6.5, we see that the difference in NOx peaks for the model and the measurement is very big for a torque step. However, in Figure 6.4 a similar torque step is made and the NOx model and the measurement show similar behaviour.

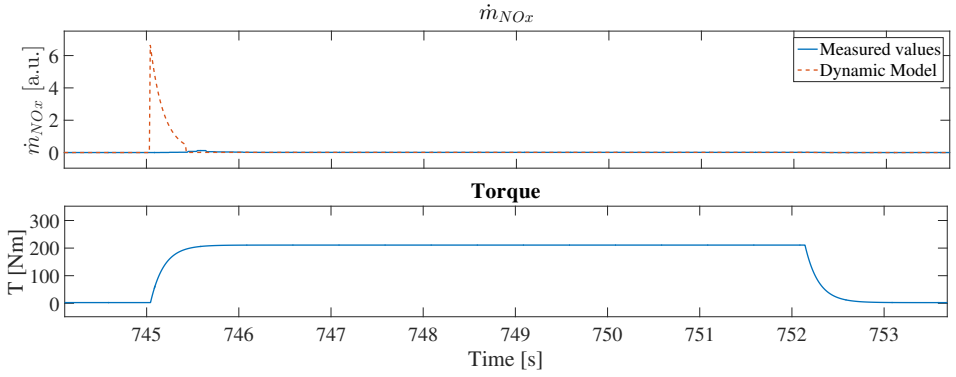

Figure 6.5: *Dynamic NOx model together with measured NOx.*

In Figure 6.6 the static NOx model and the convex static NOx model are illustrated. It is seen that the convex static model often overestimates the static model.

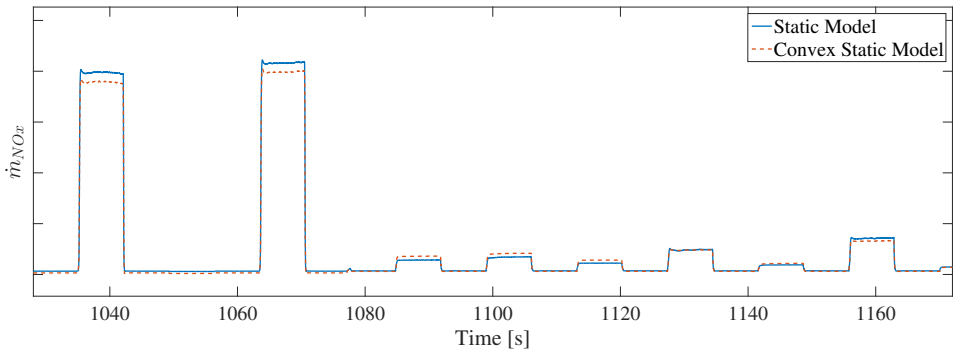

Figure 6.6: *Static NOx model and Convex Static NOx model.*

6.2 Optimization

Below, results obtained from the optimization is presented and commented to point out interesting phenomena.

The engine torque trajectories obtained from the global optimization and the MPC for a set of different prediction horizons are presented in Figure 6.7. The results are shown for only the WLTC drive cycle because the behaviour is the same for each drive cycle. Only the dynamic MPC is presented due to the solution obtained from the static MPC, independent of prediction horizon, is similar to the solution obtained from the static global optimization. In Figure 6.7 it is worth noticing the difference in how the torque is requested from the ICE and the ISG when comparing the global static solution and the dynamic global solution. Another interesting fact is how the optimization is able to use the the two actuators for different prediction horizons. Several different prediction horizons were analyzed, but to demonstrate the major characteristics the prediction horizons used in Figure 6.7 are enough. In Figure 6.8 the resulting fuel mass flow and NOx mass flow are illustrated.

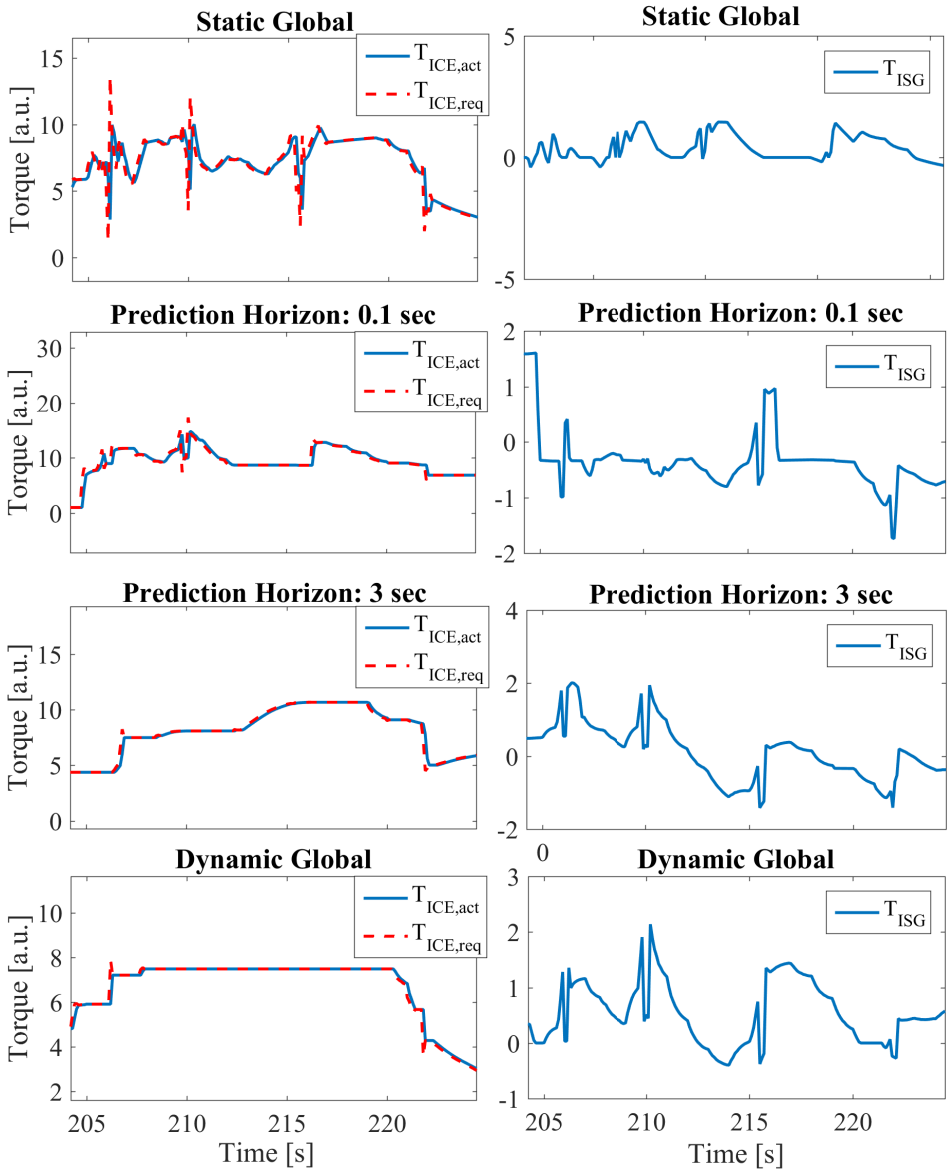

Figure 6.7: *A time slot of the WLTC drive cycle that visualizes how $T_{ICE,act}$, $T_{ICE,req}$, and T_{ISG} differ if the controller has no knowledge about the dynamic behavior (row one), has limited knowledge of the dynamics ahead (rows two and three) and when it has complete knowledge of the dynamics for the drive cycle (row four).*

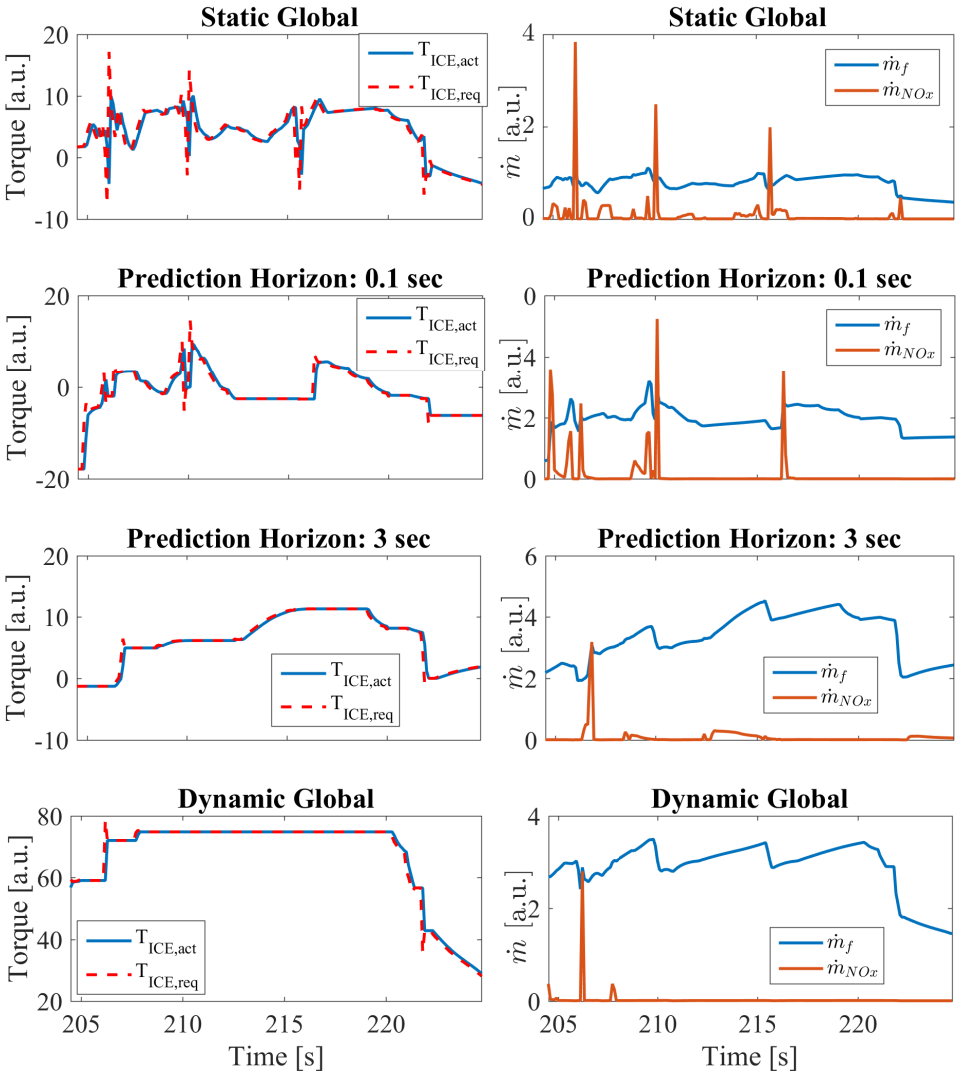

Figure 6.8: *A time slot of the WLTC drive cycle that visualizes how the fuel mass flow and NOx emissions differ if the controller has no knowledge about the dynamic behavior (row one), has limited knowledge of the dynamics ahead (rows two and three) and when it has complete knowledge of the dynamics for the drive cycle (row four).The figures to the left are the same as in Figure 6.7*

The following section presents the results of each plant and drive cycle. First, the results obtained from Plant 1 are presented and thereafter, the results for Plant 2. All the vales for the cost functions have been normalized with each drive cycles global solution, obtained from the dynamic controller.

WLTC - Plant 1

In Figure 6.9, the advantage of using a dynamic controller can be seen. The dynamic controller is able to minimize the fuel consumption and NOx emissions because the transient engine operation is better for the dynamic controller than for the static controller. The x-axis has a logarithmic scale to highlight that the major reduction of the cost function is made for small prediction horizons.

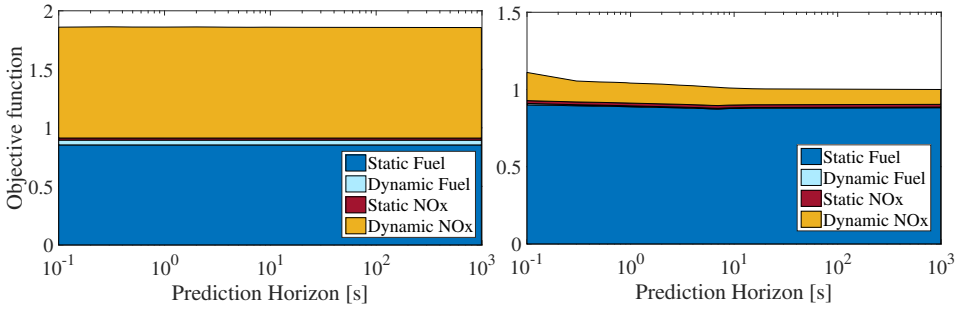

Figure 6.9: *The objective function and its individual portions as a function of prediction horizon for both the static and dynamic controller evaluated in Plant 1 for the WLTC drive cycle. The left figure represent the obtained results from the static controller and the right figure, results obtained from the dynamic controller. All values are normalized with the solution obtained from the dynamic global optimization.*

In Figure 6.10, the SoC trajectories for the dynamic controller are presented for a set of prediction horizons and for the global SoC trajectory. Note that longer prediction horizon results in a SoC trajectory favouring higher SoC values. For the static controller, no such trend is observed and the SoC trajectories do not have a considerable dependency on the prediction horizon. The SoC trajectory that differs from the other is the global SoC trajectory, see Figure 6.11.

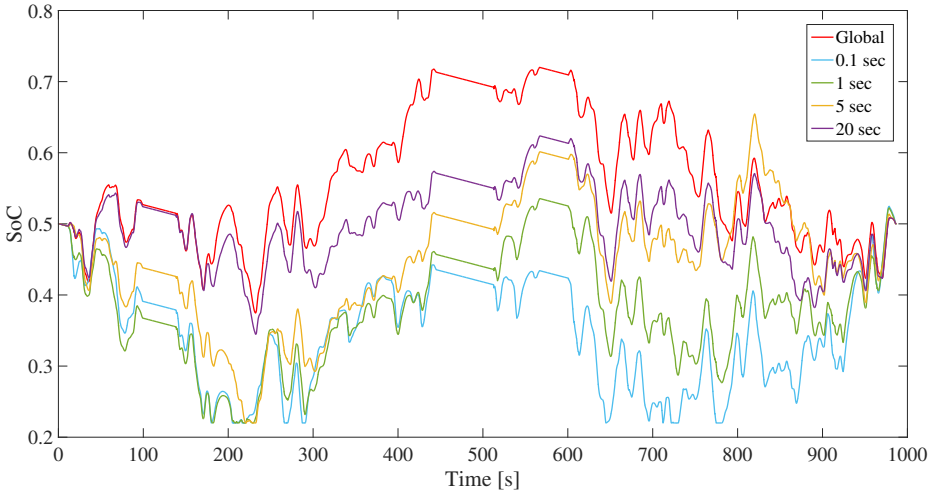

Figure 6.10: *SoC trajectory for different prediction horizons, including the global solution, using the dynamic model in the controller for the WLTC drive cycle.*

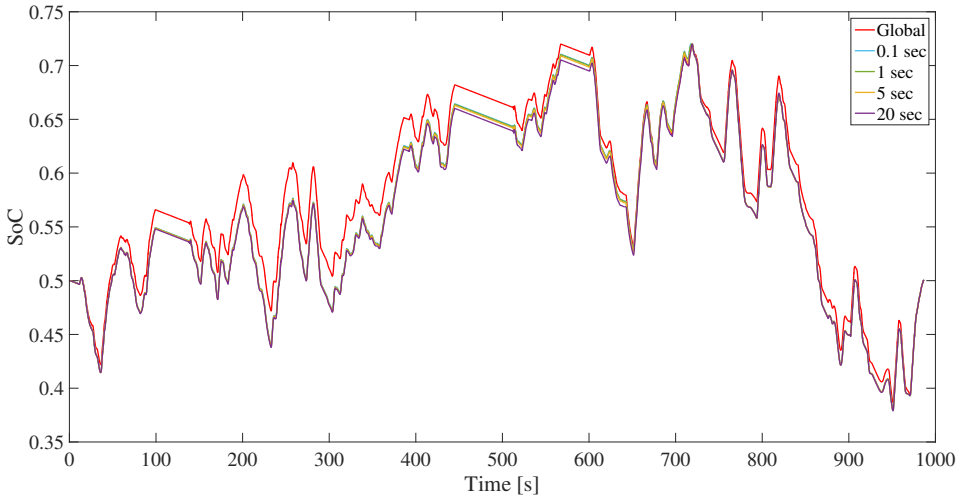

Figure 6.11: *SoC trajectory for different prediction horizons, including the global solution, using the static model in the controller for the WLTC drive cycle.*

FTP75 - Plant 1

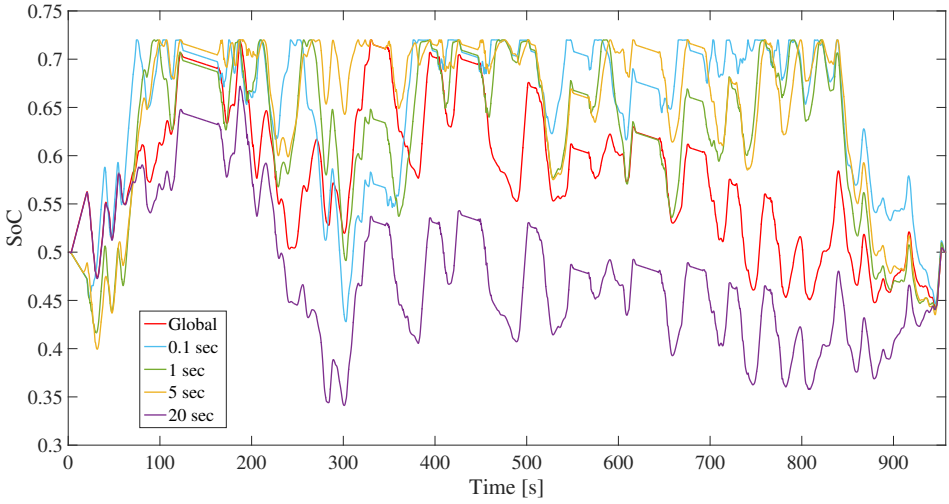

Figure 6.12: *SoC trajectory for different prediction horizons, including the global solution, using the dynamic models in the controller for FTP75.*

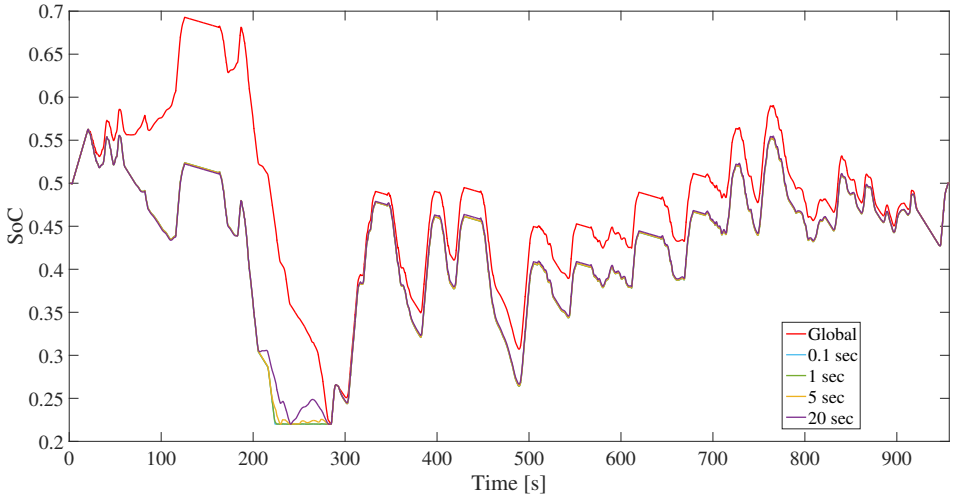

Figure 6.13: *SoC trajectory for different prediction horizons, including the global solution, using the static models in the controller for FTP75.*

When inspecting Figure 6.12, it is seen that the SoC reaches its upper limits for lower prediction horizons and when inspecting Figure 6.13, we see that the SoC

reaches its lower limits for lower prediction horizons. The SoC trajectories differ more for the dynamic controller than for the static controller. For the static controller, the biggest difference for the SoC trajectories is between the global trajectory and all others who are more or less the same independent of the length of the prediction horizon.

In Figure 6.14, the same trend as for the WLTC drive cycle is observed. However, The curve is not as smooth and this is probably due to that the solver occasionally only finds the optimal solution within reduced tolerances.

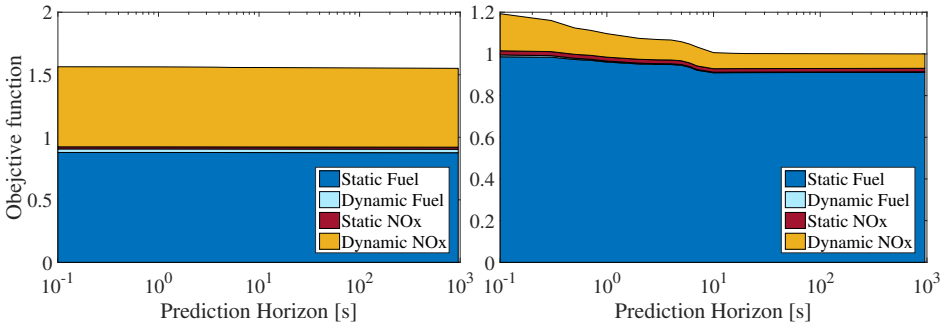

Figure 6.14: *The objective function and its individual portions as a function of prediction horizon for both the static and dynamic controller evaluated in Plant 1 for the FTP75 drive cycle. The left figure represents results obtained from the static controller and the right figure, results obtained from the dynamic controller. All values are normalized with the solution obtained from the dynamic global optimization.*

City driving cycle - Plant 1

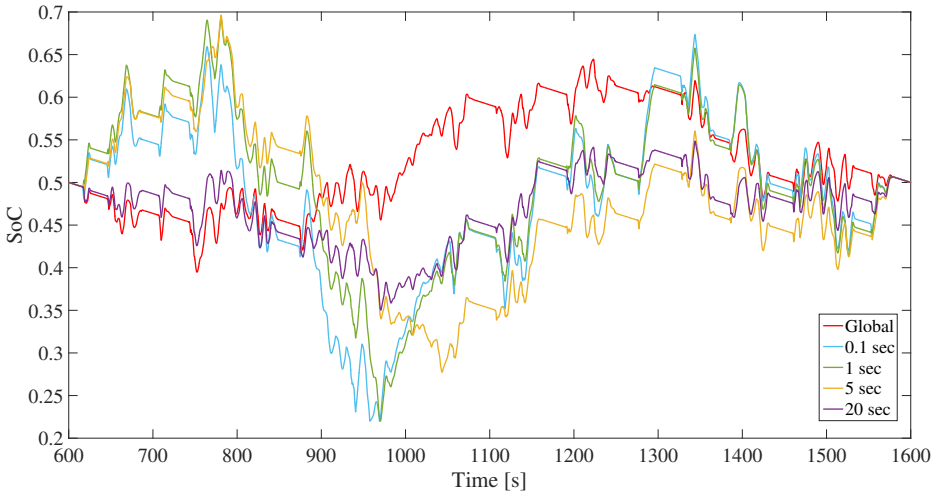

Figure 6.15: *SoC trajectory for different prediction horizons, including global solution, using the dynamic model in the controller for the City drive cycle.*

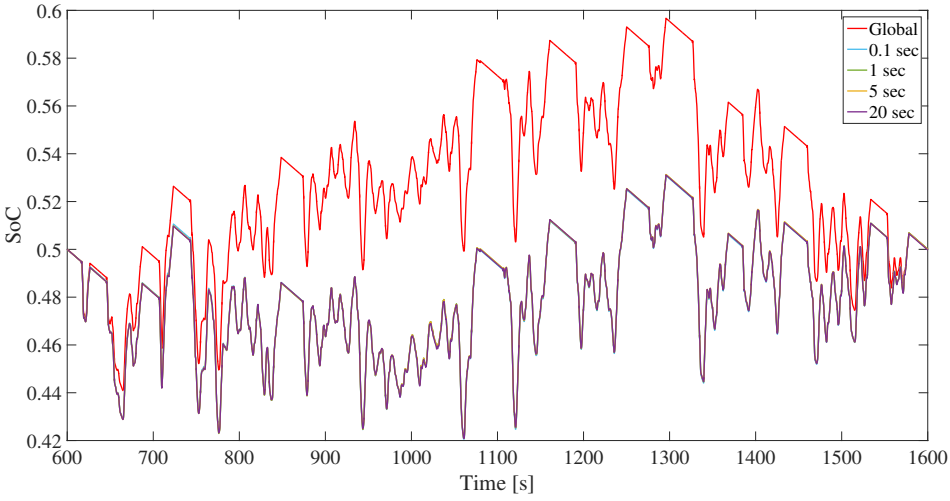

Figure 6.16: *SoC trajectory for different prediction horizons, including global solution, using the static model in the controller for the City drive cycle.*

The SoC trajectories obtained by using the static controller are visualized in Figure 6.16. Notice the difference between the global solution and the trajectories obtained using MPC with different prediction horizons.
In Figure 6.17, similar behavior is observed as for the WLTC and FTP75 drive cycles, see Figures 6.9 and 6.14. One thing that differs is the amount of dynamic NOx for the dynamic controller which is higher for the City driving cycle than for the other drive cycles. The SoC trajectory, see Figure 6.15, when using the dynamic model in the controller fluctuates more for shorter prediction horizon. For the lowest prediction horizon, the fluctuation almost reaches both the maximum and the minimum allowed SoC value.

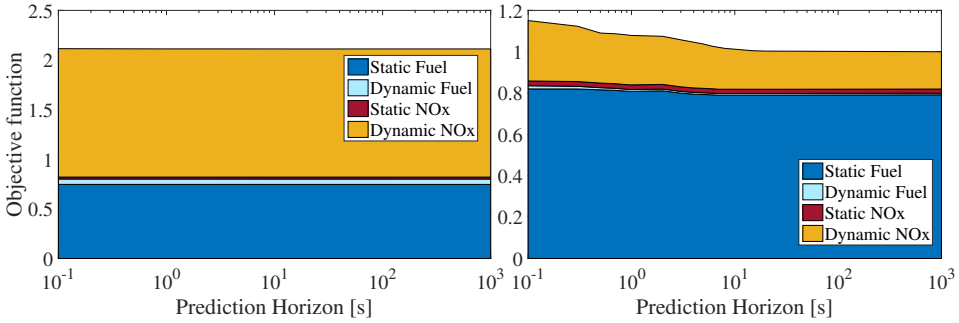

Figure 6.17: *The objective function and its individual portions as a function of prediction horizon for both the static and dynamic controller evaluated in Plant 1 for the City drive cycle. The left figure represents the obtained result from the static controller and the right shows the result obtained from the dynamic controller. All values are normalized with the solution obtained from the dynamic global optimization.*

WLTC - Plant 2

When applying the optimal torque split on Plant 2 a similar result was obtained as when applied on Plant 1. When analyzing Figure 6.18, Figure 6.19, and Figure 6.20 a difference is observed when compared to the corresponding Figures for Plant 1, see Figures 6.9, 6.14 and 6.17. This difference is because of the convex static models, used in Plant 1, are over-estimating fuel and NOx compared to the static model. Since the models describing the extra fuel consumption and NOx emissions due to transient engine operation are the same in both plants, their portion relative the global solution will be larger. All values in the following figures are normalized with the solution obtained from the dynamic global optimization.

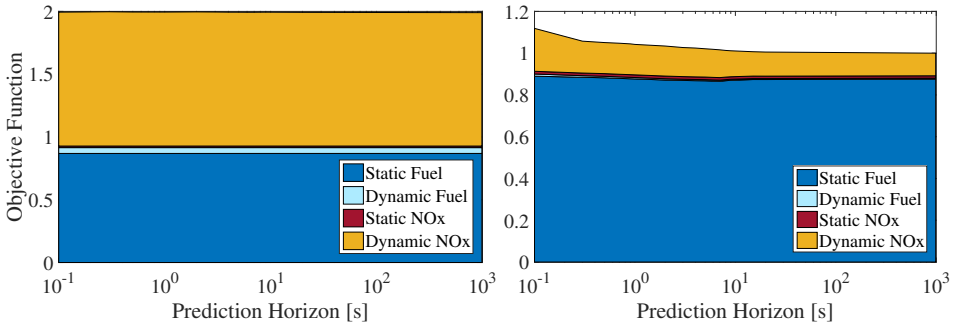

Figure 6.18: *The objective function and its individual portions as a function of the prediction horizon for both the static and dynamic controller evaluated in Plant 2 for the WLTC drive cycle. The left figure represents the results obtained from the static controller and the right figure shows the results obtained from the dynamic controller.*

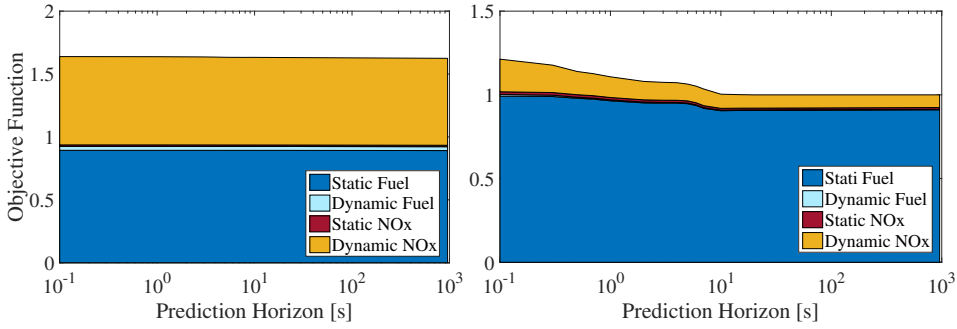

Figure 6.19: *The objective function and its individual portions as a function of the prediction horizon for both the static and dynamic controller evaluated in Plant 2 for the FTP75 drive cycle. The left figure represents the results obtained from the static controller and the right figure shows the results obtained from the dynamic controller.*

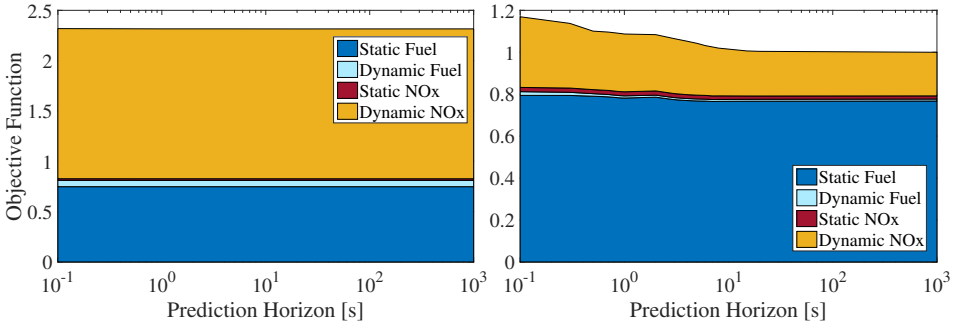

Figure 6.20: *The objective function and its individual portions as a function of prediction horizon for both the static and dynamic controller evaluated in Plant 2 for the City drive cycle. The left figure represents the results obtained from the static controller and the right figure shows the results obtained from the dynamic controller.*

Calculation Time

Another variable of interest when evaluating an MPC is the calculation time and how it differs when using different lengths of the prediction horizon. All calculations were done using a laptop with quad core i7 2.8 GHz CPU and Matlab R2015b. In Figure 6.21, it is illustrated how the calculation time depends on the length of the prediction horizon. The dependency is close to exponential and there exist some strange behaviour where the computation time decreases with longer prediction horizon. This is probably a consequence from that the optimization is able to find the solution using less iterations for some specific cases.

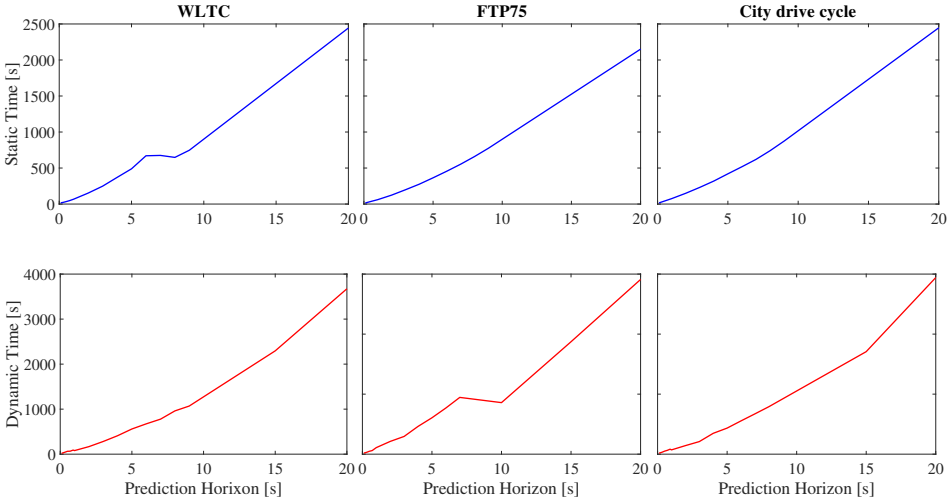

Figure 6.21: *Calculation time for the MPC as a function of the length of the prediction horizon for the three investigated drive cycles. The top row represents the static controller and the bottom row shows the dynamic controller. Each column corresponds to one drive cycle.*

7

Analyses of Result

In this chapter the results presented in the previous chapter are discussed and analyzed. First the models are analyzed and then the different optimization methods will be investigated.

7.1 Models

The decision to use convex optimization implied developing convex model approximations of the non-convex models. By using convex static models instead of static models, bigger model errors are introduced due to another model approximation. This applies for all the convex models and is presented in section 6.1 for the NOx and fuel models. The relative mean errors for the convex fuel and convex NOx model turned out to be bigger than expected, especially for NOx. However, the mean is highly affected by a few huge relative errors occurring for negative and positive torques close to zero. This is confirmed when considering only positive engine torques above 15 Nm. Then, the relative mean error is reduced for both fuel and NOx, as seen when comparing Table 6.2 and Table 6.4.

However, one can not neglect some torques and the method used for approximating the static fuel and NOx map would have to be improved to get a better convex approximation. Also, note that the error for the non-convex dynamic fuel model is lower than for the non-convex static fuel model, see Tables 6.2 and 6.3, indicating that the dynamic fuel model is a good approach and that the problem is with the convex static models.

Also worth mentioning is that the dynamic model for NOx is not always able to correlate NOx peaks to torque steps as seen in the measurement data. An example is illustrated in Figure 6.5. This is because the data used for validating the

NOx model was obtained from measurements in which several parameters were adjusted in order to develop a more complex NOx model. To be able to capture this behaviour, these parameters have to be taken into account which is beyond the scope of this thesis. However, the model developed in the thesis could probably be tuned better if better measurement data had been available. That is, if the data had been produced for the purpose of this thesis.

By comparing the cost function evaluated in Plant 1 and Plant 2, it can be seen that the errors due to convex approximation do not have a big impact on how the MPC is able to minimize the cost function with increasing prediction horizon. Even though the behaviour is the same, the values of the cost function differ quite a lot for Plant 1 and Plant 2 and this is because of the convex models often overestimating the static models.

7.2 Optimization

By studying Figures 6.7 and 6.8, the difference between how the different controllers uses the ICE and the ISG is illustrated. The dynamic optimization tries to run the ICE at steady state engine operation as much as possible in order to avoid extra fuel consumption and emissions due to transient engine operation. Instead, it utilizes the ISG to minimize transient engine operation in order to cancel out the resulting consequences. This phenomena increases with the length of the prediction horizon. The MPC with a 0.1 second long prediction horizon is not able to counteract the engine dynamics as well as the MPC with a prediction horizon of 3 seconds. This is due to the fact that the time constant of the dominating dynamics of the ICE (the turbo-lag) is higher than 0.1 seconds and lower than 3 seconds. The resulting fuel consumption and NOx emissions are presented in Figure 6.8 where it is seen that the ability to decrease the amount of fuel and NOx peaks increase with a longer prediction horizon for the dynamic controller.

This is also confirmed in Figures 6.9 and 6.17 where a decreasing trend of the cost function with increasing prediction horizon is observed for the dynamic controller for each drive cycle which is consistent with the behaviour of the actuators, as explained above. However, the drawbacks of the dynamic NOx model developed are again illustrated. When the dynamics are not taken into account, as for the static controller, the dynamic NOx represent approximately half of the total value of the cost function, or in other words, it represents the cost of static fuel, dynamic fuel and static NOx together. This does not represent reality and is either a consequence of having insufficient data when constructing the simple model or not having a more complete model. This must be further investigated.

One could question why a more complex model was not developed in this thesis and there are three major reasons why not. Firstly, since most EMS that are used today do not incorporate dynamic models for either fuel or NOx, the aim of this thesis was to investigate if by doing so, could some improvements be made.

Therefore, a simple model was the natural approach to begin with. Secondly, the long term goal of the developed MPC is to be implemented on an Electronic Control Unit (ECU). An ECU has very limited computing power and therefore, a simple model should be used. Thirdly, developing a more complex NOx model would be a thesis work by itself and is outside the scope of this thesis. Therefore, the approach that has been used here is considered appropriate.

Nonetheless, the developed EMS behaves very well and is able to decrease fuel consumption and NOx emissions due to transient engine operation. Even though the major effect is seen for dynamic NOx, it is also able to decrease dynamic fuel consumption while keeping the static fuel consumption and NOx emissions around the same level as the static controller. This is observed for both Plant 1 and Plant 2, meaning that the model errors introduced through convex approximation do not cause different behaviour. However, since the dynamic part of the developed models are the same in the controller as for both Plant 1 and Plant 2, further validation would be needed to fully confirm this.

Worth noticing is that the static controller is not able to reduce the value of the cost function when the prediction horizon is increased. By studying Figures 6.10 and 6.17, it is identified that the value of the cost function is more or less constant; in other words, it is independent of the length of the prediction horizon. There is a slight decreasing trend toward the global solution but it is negligible. This is also confirmed when studying the SoC trajectories for the static controller, see Figures 6.11, 6.13 and 6.16. The SoC trajectory is not dependent on the prediction horizon and the only noticeable difference is that the global solution finds a different SoC trajectory than the static MPC. This is reasonable since the global solution is able to vary λ_{ech}, while it is a constant value for the MPC. The value resulting in a charge sustaining trajectory. However, the behaviour of the static MPC, primarily the solution being independent of the length of the prediction horizon should be investigated further.

The SoC trajectory for the dynamic controller differs a lot, more than for the static controller. This is reasonable because it is able to predict and counteract transient engine operation by using the ISG in a more efficient way in this context. By changing the behaviour of the ISG which directly affects how the battery is charged/discharged, the SoC trajectory will be affected as well. Another trend that is present when investigating the SoC trajectories is that the global solution favours higher levels of the SoC, meaning that its trajectory finds a higher SoC value then what the solution using a prediction horizon has. One reason for this could be that since the battery losses depend on SoC level according to Equation 4.17, a higher level of SoC will result in lower battery losses which in turn results in a more efficient way of using the battery to reduce fuel consumption and NOx emissions. The global optimization has the flexibility to vary λ_{NOx} during the cycle, and utilizes this to achieve battery operation in a higher SoC range. The MPC controller is limited to one constant lambda value throughout the entire cycle, hence lacks this flexibility.

However, the results are somewhat misguiding. The choice of a constant lambda without a more sophisticated SoC controller might lead to what is illustrated in Figure 6.10 and Figures 6.12 and 6.13. That is, without a more sophisticated SoC controller, the choice of a constant lambda could potentially lead to the SoC trajectory reaching the SoC limits many times during a drive cycle. Consequently, the free energy gained from regenerative braking can not be utilized if the battery is fully charged when this occurs, or if the battery is fully depleted, the ICE would have to be used if the driver would accelerate the vehicle heavily, which results in transient engine operation that could have been avoided.

In Figure 6.21, the computing time as a function of the length of the prediction horizon is presented for the static and dynamic MPC, and for each drive cycle. It is seen that the relationship is almost exponential but for low prediction horizons the MPC is quite fast. This in combination with that the major improvement in reduction of the cost function is achieved for short predictions horizons is a positive result. If the MPC were to be implemented on an ECU, a short prediction horizon would be a requirement for the MPC.

8

Conclusions & Future Work

8.1 Conclusions

The conclusions drawn in this chapter answer the posed thesis questions, see section 1.6, and are based on the results in chapter 6 and analyses made in chapter 7.

- It is possible to save fuel and reduce NOx emissions when using a controller that incorporates simple models of NOx emissions and fuel consumption due to transient engine operation. The NOx peaks can be very high during transients relative to the magnitude of NOx emissions during steady-state engine operation, as can be seen in the measurement data in [13]. Therefore, a model capturing this behaviour is considered to be a better approximation of reality than a model that only considers steady state engine operation.
- When implementing a dynamic MPC, it is observed that the ability to decrease NOx emissions and fuel consumption increases with the length of the prediction horizon. Note that the major improvement is made for small prediction horizons, 0.1 to 1 seconds, and that no major improvement is seen after 10 seconds for all drive cycles investigated in this thesis. It is very good that the biggest improvement is made for very low prediction horizons because if an MPC is implemented on an ECU, the requirement on computational efficiency would only make an MPC with very small prediction horizon possible for implementation.
- The computational time for the developed MPC increases with increasing prediction horizon. This relationship is close to exponential. However, not a lot of effort have been put into making the MPC as computationally efficient as possible and the code could be improved in this context.

- The optimization was investigated using two different plants, one with the same models used in the controller and one with different static models. When the optimal torque split is validated using both plants, similar results are obtained indicating that the model errors due to convex approximation do not have a major impact on the how the MPC is able to reduce fuel consumption and NOx emissions with an increased prediction horizon. This is positive since none of the models that are being used today is able to represent reality without any errors. However, the value of the cost function evaluated in Plant 1 and Plant 2 differs quite a bit and it is because of the bad convex approximation of the static maps.

8.2 Future Work

In this chapter, suggestions are made on how the work in this thesis can be further developed. Some improvements that can be made on the work done in this thesis are also discussed.

To obtain a better approximation of the static models, the convex static models can be improved. As the majority of the errors occur for engine torques around zero and below, the biggest improvement can be made for those cases.

The developed transient NOx model does not represent reality very well. As explained earlier, this is due to that the measurement data that was used for developing the model was intended for the development of another NOx model, and takes more parameters into account when it estimates NOx emissions. It would be interesting to see if the model that was developed in this thesis could be tuned better if better measurement data was available. Especially since the optimization does a very good job when minimizing transient engine operation if the fuel consumption and NOx emissions due to transients can be expressed as function of the difference between requested torque and actual torque. If using better measurement still does not result in a good dynamic NOx model, a more complex model must be investigated.

In this thesis, piecewise linearization was used to get convex models. Some models could be approximated using a quadratic function. It would be interesting to investigate the trade off in accuracy and computing time of the optimization for these two approaches. As a first step, the battery losses, that in this thesis was approximated using a second order cone, could be compared with a model approximation using piecewise linearization.

A more sophisticated SoC controller would be favourable to implement along side the MPC. This is because the constant lambda approach without a SoC controller might result in the battery reaching its limits during scenarios where it would be favourable to be able to discharge the battery further or charge it more. This investigation might give a better understanding about how different predic-

tion horizons correlates to the SoC trajectory, especially for the static MPC.

The MPC would have to be applied on a much more complex car model with a driver model to be able to really understand how it would perform in reality. A good next step would be to implement the MPC in VSim where complex vehicle models as well as driver models already have been implemented.

Not a lot of effort has been focused on making the code more efficient and it would be interesting to see if improvements in computational time could be made by doing so. Writing the MPC in a faster programming language such as C would also be of interest. By decreasing the computational time a longer prediction horizon could be possible when implementing the MPC on an ECU.

Appendices

A

Drive Cycles

In this appendix drive cycles used in the thesis are presented. The drive cycles are used to validate the result of the models and the MPC.

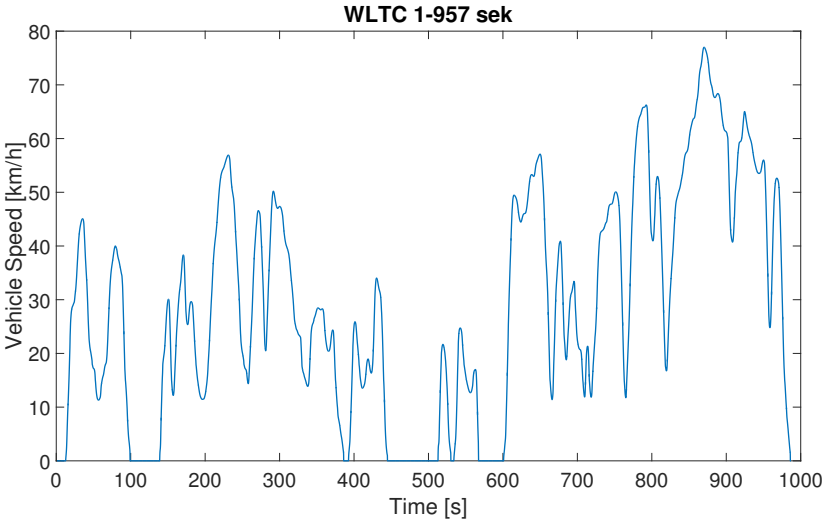

Figure A.1: *Velocity profile for WLTC*

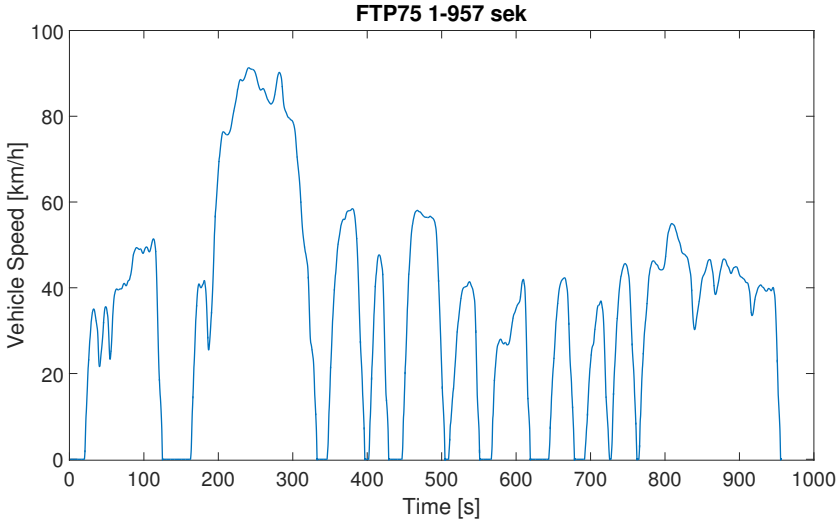

Figure A.2: *Velocity profile for FTP75*

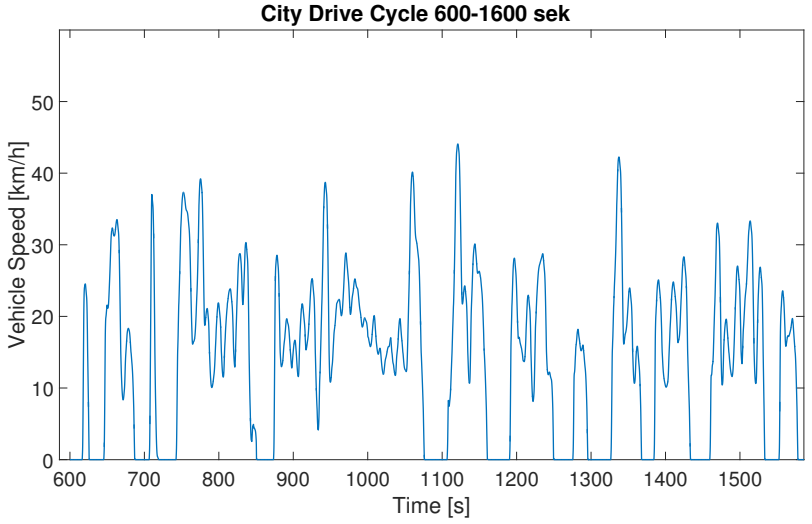

Figure A.3: *Velocity profile for a random drive cycle from city driving*

B

Tables

Data from the MPC are presented in a table for the WLTC using Plant 1. Here, the values of the results shown in Figure 6.9 are presented. The calculation time (**Time**) is normalized using the calculation time for MPC with a prediction horizon of 0.1 for the static and the dynamic models. Meaning that with a longer prediction horizon, the calculation time increases with the calculation time at prediction horizon 0.1 times the time value at the corresponding prediction horizon.

PH, Static [s]	$J_{f,stat}$	$J_{f,dyn}$	$J_{NOx,stat}$	$J_{NOx,dyn}$	J_{tot}	Time
0.1	0.8541	0.04117	0.01773	0.9472	1.86	1
0.3	0.8541	0.04127	0.01773	0.9501	1.863	1.4384
0.5	0.8541	0.0412	0.01773	0.9482	1.861	2.0707
0.7	0.8541	0.0412	0.01773	0.948	1.861	2.7331
1	0.8541	0.04119	0.01773	0.9478	1.861	3.9853
2	0.854	0.04122	0.01773	0.9491	1.862	8.9483
3	0.854	0.04119	0.01773	0.9481	1.861	14.6026
4	0.854	0.04116	0.01773	0.947	1.86	21.7489
5	0.854	0.04116	0.01773	0.9468	1.86	28.7813
6	0.854	0.04114	0.01773	0.9463	1.859	39.4300
7	0.854	0.04115	0.01773	0.9464	1.859	39.7237
8	0.854	0.04117	0.01773	0.9468	1.86	38.1137
9	0.854	0.04118	0.01773	0.947	1.86	43.9602
Global	0.8539	0.04103	0.01776	0.944	1.857	20.9736

PH, Dynamic [s]	$J_{f,stat}$	$J_{f,dyn}$	$J_{NOx,stat}$	$J_{NOx,dyn}$	J_{tot}	Time
0.1	0.9005	0.00954	0.01805	0.1826	1.11	1
0.3	0.8947	0.006703	0.01789	0.1356	1.055	2.0847
0.5	0.8925	0.06333	0.01792	0.1321	1.049	3.3037
0.7	0.8904	0.006246	0.01791	0.132	1.047	3.4635
1	0.8881	0.005927	0.01794	0.1295	1.041	4.1543
2	0.8836	0.005448	0.01797	0.1278	1.035	8.7167
3	0.8812	0.005029	0.01795	0.1237	1.028	14.6904
4	0.8787	0.004929	0.01793	0.1227	1.024	21.3444
5	0.8769	0.004829	0.01788	0.1203	1.02	29.1513
6	0.8746	0.004804	0.01778	0.1194	1.017	35.0947
7	0.8734	0.004751	0.01772	0.1181	1.014	40.5529
8	0.8755	0.004556	0.01774	0.1135	1.011	50.0862
9	0.8769	0.004442	0.01775	0.1105	1.01	55.7240
15	0.8791	0.004222	0.01784	0.1037	1.005	119.6217
20	0.8792	0.00421	0.0178	0.1024	1.004	191.4819
Global	0.882	0.004081	0.01767	0.09623	1	224.0329

Table B.1: *The distribution of cost for the real-time optimizer using the static model and the dynamic model respectively for different Prediction Horizons (PH). Also the calculation time for each PH is presented in the right column. The data is taken from the WLTC, and is the same as Figure 6.9.*

Bibliography

[1] Carole Quérel Olivier Grondin, Laurent Thibault. Energy Management Strategies for Diesel Hybrid Electric Vehicle. *Oil Gas Sci. Technol*, 70:125–141, 2015. Cited on page 2.

[2] Tobias Nüesch Mu Wang Christoph Voser and Lino Guzzella. Optimal energy management and sizing for hybrid electric vehicles considering transient emissions. *IFAC Workshop on Engine and Powertrain Control*, 45(30): 278–285, Rueil-Malmaison France 2012. Cited on pages 5, 6, 27, and 28.

[3] Fengjun Yan Junmin Wang and Kaisheng Huang. Hybrid electric vehicle model predictive control torque-split strategy incorporating engine transient characteristics. *IEEE Transactions on Vehicular Technology*, 61(6), 2012. Cited on pages 2, 4, 5, and 27.

[4] Aishwarya Panday and Hari Om Bansal. A review of optimal energy management strategies for hybrid electric vehicle. *International Journal of Vehicular Technology*, 2014, 2014. Cited on pages 2, 4, and 5.

[5] Lino Guzella and Antonio Sciarretta. *Vehicle Propulsion System*. Springer, third edition, 2013. Cited on pages 2, 6, 12, 13, 14, 16, and 17.

[6] Namwook Kim Sukwon Cha and Huei Peng. Optimal control of hybrid electric vehicles based on pontryagin's minimum principle. *IEEE Transactions on Control Systems Technology*, 19(5):1279–1287, 2011. Cited on pages 4 and 5.

[7] Lorenzo Serrao and Giorgio Rizzoni. Optimal control of power split for a hybrid electric refuse vehicle. *Proceedings of the American Control Conference*, pages 4498–4503, 2008. Cited on pages 4 and 5.

[8] G. Paganelli M. Tateno A. Brahma G. Rizzoni and Y. Guezennec. Control development for a hybrid-electric sport-utility vehicle: strategy, implementation and field test results. *American Control Conference*, 2001. Cited on page 4.

[9] Valerie H. Johnsson Keith B. Wipke and David J. Rausen. Hev control strategy for real-time optimization of fuel economy and emissions. *Society of Automotive Engineers, Inc, Future Car Congress 2000-01-1543*, Arlington, Virginia, 2000. Cited on page 4.

[10] Tobias Nüesch Philipp Ebert Michael Flankl Christopher Onder and Lino Guzzella. Convex optimization for the energy management of hybrid electric vehicles considering engine start and gearshift costs. *Elsevier*, 7(2): 834–856, Switzerland, Europe: Multidisciplinary Digital Publishing Institute 2014. Cited on page 5.

[11] Vaheed Nezhadali Martin Sivertsson and Lars Eriksson. Turbocharger dynamics influence on optimal control of diesel engine powered systems. *SAE International Journal of Engines 2014-01-0290*, 7(1), Linköping University, 2014. Cited on pages 5 and 27.

[12] William Glewen David Heuwetter David Foster Michael Andrie and Roger Krieger. Analysis of deviations from steady state performance during transient operation of a light duty diesel engine. *SAE International Journal of Engines 2012-01-1067*, 5(3):909–922, University of Wisconsin, 2012. Cited on page 5.

[13] Dihnesh V Velmurugan Markus Grahn and Tomas McKelvey. Diesel engine emission model transient cycle validation. *International Federation of Automatic Control*, 49(11), 2016. Cited on pages 5, 6, 7, 8, 25, 26, 27, 29, 42, 43, and 67.

[14] Markus Grahn Krister Johannson and Tomas McKelvey. Model-based diesel engine management system optimization for transient engine operation. *Elsevier, Control Engineering Practice*, 29:103–114, Chalmers University of Technology Department of Signals and Systems, Signal Processing 2014. Cited on page 6.

[15] Kaj Holmberg. *Optimering*. Liber AB, first edition, 2010. Cited on page 15.

[16] Christopher Onder Stephan Zentner, Jonas Asprion and Lino Guzzella. An Equivalent Emission Minimization Strategy for Causal Optimal Control of Diesel Engines. *Energies*, 7:1230–1250, 2014. Cited on pages 16 and 17.

[17] Viktor Larsson. Route Optimized Energy Management of Plug-in Hybrid Electric Vehicles. *Ph.D, Chalmers University of Technology*, 2014. Cited on page 17.

[18] Stephen Boyd and Lieven Vandenberghe. *Convex Optimization*. Cambridge University Press, seventh edition, 2004. Cited on page 18.

[19] A. Domahidi, E. Chu, and S. Boyd. ECOS: An SOCP solver for embedded systems. In *European Control Conference (ECC)*, pages 3071–3076, 2013. Cited on page 19.

[20] Miguel Sousa Lobo, Lieven Vandenberghe, Hervé Lebret, and Stephen Boyd. Applications of second-order cone programming. *Elsevier Science Inc, Linear Algebra and Applications*, 284(1–3):193–228, D.P. O'Leary 1998. Cited on page 20.

[21] Yi Huo and Fengjun Yan. A predictive energy management strategy for hybrid electric powertrain with a turbocharged diesel engine. *Journal of Dynamic Systems, Measurement and Control*, 2017. Cited on page 20.

[22] Martin Enqvist, Torkel Glad, Svante Gunnarsson, Peter Lindskog, Lennart Ljung, Johan Löfberg, Tomas McKelvey, Anders Stenman, and Jan-Erik Strömberg. *Industriell reglerteknik Kurskompendium*. Linköpings Universitet, first edition, 2014. Cited on page 20.

[23] Monica Tutuianu, Alessandro Marotta, Heinz Steven, Eva Ericsson, Takahiro Haniu, Noriyuki Ichikawa, and Hajime Ishii. Development of a World-wide Worldwide harmonized Light duty driving Test Cycle (WLTC). Technical report, 12 2013. Cited on page 22.

[24] Parthasarathy Gomadam, John Weidner, Roger Dougal, and Ralph White. Mathematical modeling of lithium-ion and nickel battery systems. *Elsevier, Journal of Power Sources*, 110(2):267–284, United States, North America: Scholar Commons, 2002. Cited on page 23.

[25] Xiaosong Hua, Shengbo Li, and Huei Penga. A comparative study of equivalent circuit models for li-ion batteries. *Journal of Power Sources*, 2012. Cited on page 23.

[26] Michael Grant and Stephen Boyd. Qcml version 0.2.0. a python toolbox for matrix stuffing. `https://github.com/cvxgrp/qcml`, November 2014. Cited on page 39.